Electronic Supplementary Material (ESI) for Chemical Communications.

Electronic Supplementary Information

DNA Labelling in Live Cells via Visible Light-Induced [2+2] Photo-cycloaddition

Rita T. Michenfelder, Laura Delafresnaye, Vinh X. Truong*, Christopher Barner-Kowollik* and Hans-Achim Wagenknecht*

Abstract: We introduce a visible light-driven (λ_{max}=451 nm) photo-chemical strategy for labelling of DNA in living HeLa cells *via* the [2+2] cycloaddition of a styrylquinoxaline moiety, which we incorporate into both the DNA and the fluorescent label. Our methodology offers advanced opportunities for the mild remote labelling of DNA in water while avoiding UV light activation.

Table of Contents

1 Materials and Methods

All reactions were either performed under a dry argon environment or under inert atmosphere, as detailed for each reaction in Chapter 2 (Synthetic Procedures). All solvents and reagents were commercially purchased at ABCR, ACROS Organics, ALFA Aesar, Carl Roth, Merck, Sigma Aldrich and VWR. Unless stated otherwise, all chemicals were used as received without further purification. Anhydrous solvents were purchased at ACROS Organics and stored under argon. HPLC grade solvents were acquired at Fisher Scientific, deuterated solvents for NMR spectroscopy were purchased at Eurisotop. Water was deionized using a Merck Millipore-Q8. Concerning reactions under inert conditions, flasks and other glassware were heated with a heat gun and dried in high vacuum, followed by flooding with argon (99.999% purity). Room temperature refers to ambient temperature (20-22 °C). The silica gel for flash chromatography (pore size 60 Å, particle size 40-63 µM) was purchased at Sigma Aldrich. The crude product was either dissolved in the solvent system or adsorbed onto silica before purification. Pressure was applied to the column using an air pump. Reactions were monitored by Thin Layer Chromatography (TLC) using silica gel 60 F_{254} coated aluminum plates by Merck. For detection, λ=254 nm (fluorescence deletion) or λ=366 nm (fluorescence excitation) was used. For staining, 5 % H_2SO_4 in MeOH, $KMnO_4$ solution (1.50 $KMnO_4$, 10.0 g K_2CO_3, 1.85 mL 10 % NaOH and 200 mL H_2O) or 0.5 % Ninhydrin in Butan-1-ol (spray reagent) were used.

Spectroscopy

UV/Vis spectroscopy

UV/Vis absorbance was measured using 1 cm quartz glass cuvettes (Starna) with either a sample volume of 500 µL or 1 mL at 20 °C and on a Cary 100 Scan UV/Vis spectrometer (Varian).

NMR spectroscopy

NMR spectroscopic data were recorded on a Bruker Avance 400 MHz spectrometer at ambient temperature. 10 mg of compound was dissolved in 400 µL deuterated solvent. The chemical shifts are reported in δ units, parts per million (ppm) downfield from TMS. Coupling constants (*J*) are given in Hertz (Hz) and multiplicities are abbreviated as following: s (singlet), d (doublet), t (triplet), dd (doublet of doublets), td (triplet of doublets), ddd (doublet of doublet of doublets), tt (triplet of triplets), p (pentet), m (multiplet), b (broad). Various 2D technique experiments were used to establish the structures and to assign the signals.

Mass spectrometry

MALDI-TOF

Matrix-assisted laser desorption ionization (MALDI) mass spectrometry was performed on a Shimadzu Axima Confidence in reflectron (nucleosides and other small molecules) or linear negative (oligonucleotides) mode. THAP (6-Aza-2-thiothymine, saturated in MeCN) and 2,4,6-trihydroxyacetophenone (0.3 M in EtOH) or ATT (3-Hydroxypicolinic acid, saturated in MeCN/H_2O 1:1/ di-ammonium hydrogen citrate (0.44 M in H_2O) 9:1) were used as matrices.

HR-ESI

High-resolution mass spectra were obtained with an electrospray ionization Thermo Exactive orbitrap mass spectrometer.

Oligonucleotide Synthesis

Oligonucleotide synthesis was performed on a H-6 synthesizer by K&A Laborgeraete. After cleavage, the oligonucleotides were purified on a semi/preparative reversed-phase HPLC Thermo Fisher system (RP-C18 column, A = NH_4OAc buffer, B = MeCN). The purified oligonucleotide strands were quantified photometrically using a NanoDrop ND-1000 spectrometer.

Freeze Drying

For removal of water or ammonium hydroxide from the oligonucleotide samples, a Christ Alpha RVC vacuum centrifuge was used in either of the following settings: 35 min, 35 °C, 100 mbar (ammonium hydroxide) or ∞ min, 25 °C, 0.100 mbar (water).

HPLC

HPLC separation was performed on a ThermoFisher Scientific UltiMate™ 3000 system. For semi-preparative separations (DNA purification), a VDSpher OptiBio Pur 300 S18-SE column (250×10 mm, 5 µm) was employed using a flow rate of 2.5 mL min^{-1}. Elution of the product was executed through 0-20% MeCN in NH_4OAc buffer at 40 °C in 30 min, followed by 10 min hold. Analytical separations were performed using a VDSpher OptiBio Pur 300 S18-SE column (250×4.6 mm, 5 µm) with a flow rate of 1.0 mL min^{-1}. Elution of the product was executed through 0-50 % MeCN in NH_4OAc buffer at 40 °C in 30 min, followed by 10 min hold.

Irradiation experiments

Irradiation experiments were performed using 50 µM **DNA2** and 50 µM / 250 µM SQ-modified Atto dye **2** in H_2O, 10 mM Na-P_i buffer and 250 mM NaCl in a total volume of 600 µL in a crimp vial with 450 nm (**Figure S1**A) LEDs (Osram Duris E2835, GD JTLPS1.14). Irradiation was carried out using a setup which was designed and manufactured by the University of Regensburg and the workshop of the Institute for Physical Chemistry at KIT (**Figure S1**B). The mixture was irradiated from the bottom of the vial under continuous stirring and constant temperature of either 20 °C or 37 °C. Cooling or heating of the reaction was performed using a Lauda Alpha R8 thermostat.

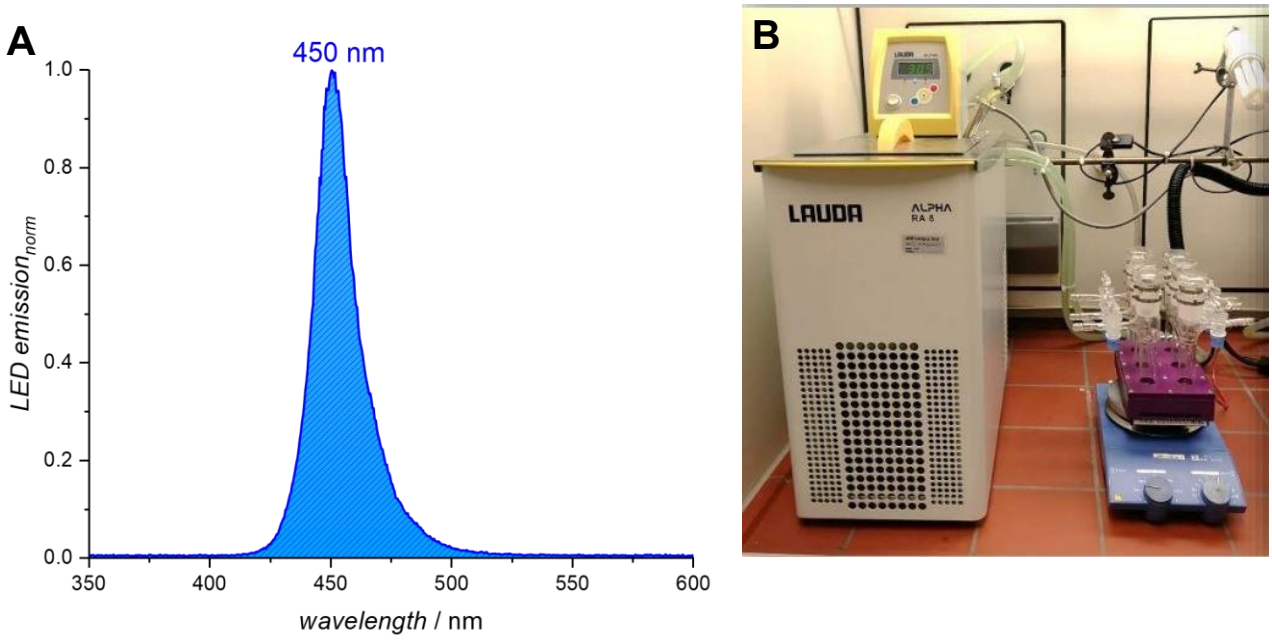

Figure S1: A: Normalised emission spectra of used LED with λ_{max} = 451 nm; **B:** Irradiation set-up with thermostat, magnetic stirrer and crimp vial rack.

Gel electrophoresis

Agarose gel electrophoresis

Agarose gel electrophoresis was performed using a PerfectBlue gel system (Mini L) by VWR Peqlab (120 V, max. 500 mA, 3 h). For gel preparation, 8.00 g agarose were diluted in 200 mL TAE buffer (40 mM tris base, 20 mM acetate and 1 mM EDTA) in a microwave until no air bubbles and smears were visible. 15 µL SybrGreen™ Nucleic Acid Gel Stain was added to the gel mixture and mixed thoroughly. The gel was poured into the gel chamber and allowed to polymerize for 1 h. Subsequently, samples were prepared using 2 µL 25 µM DNA, 8 µL ddH_2O and 2 µL loading dye (14 mM EDTA, 63 mM tris base, 63 mM boronic acid, 2.8% ficoll, 0.07% bromphenol blue, 0.01% xylene cyano FF, 5M urea) and filling the whole mixture into the gel pocket. The gel was run for 3 h (120 V, max. 500 mA) prior to imaging with a UV-light table (Raytest Bioimaging, λ_{exc}=312 nm).

Denaturing polyacrylamide/urea gel electrophoresis (PAGE)

PAGE was performed using a Sequi/Gen GT sequencing cell (21×40 cm) with a PowerPac HV. 50 mL polyacrylamide gel (12.5%) containing 16 mL acrylamide/bisacrylamide (19:1) gel mixture, 25 g urea, 5 mL ddH_2O, 89 mM tris base, 89 mM boronic acid and 20 µL TEMED were polymerized for 45 min by the addition of 425 µL ammonium persulfate (APS) solution (100 mg APS in 900 µL ddH_2O) as a radical source. A freshly prepared TBE buffer (89 mM tris base, 89 mM boronic acid, 2 mM EDTA, pH 8.0) was used as electrolyte. For sample preparation, 10 µL of 50 µM DNA solution were thinned in 10 µL ddH_2O and mixed thoroughly with 20 µL loading dye. 10 µL of the sample were filled into the gel pockets. After running the gel for 90 min at 50 °C (U = 3000 V, P = 50 W), the power source was turned off and the gel stained with SybrGreen™ Nucleic Acid Gel Stain according to the protocol supplied by the manufacturer: a mixture of 200 mg EDTA, 1.40 g boronic acid, 3.00 g tris base and 25 µL SybrGreen™ concentrate in 500 mL ddH_2O. The gel was incubated with the SybrGreen™ mixture for 30 min prior to fluorescence measurement with a Stella 830 Raytest spectrofluorometer containing LEDs radiating with a wavelength of 470 ± 10 nm or using a UV table (Raytest Bioimaging, λ_{exc}=312 nm).

2 Synthetic procedures

2.1 Synthesis of Compound 1

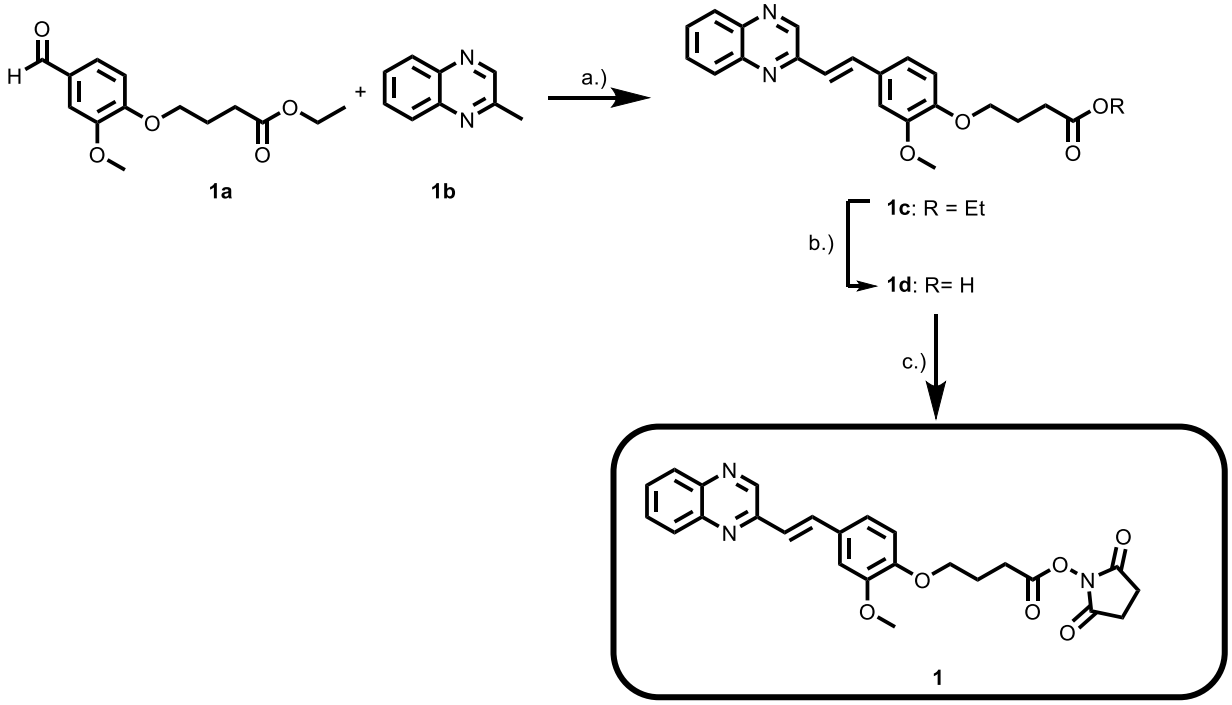

Scheme S1: Synthesis of styrylquinoxaline NHS ester **1**: a.) Acetic acid, piperidine, toluene, 115 °C, 48 h, 71%; b.) LiOH, THF, rt, 3 h, 81%; c.) EDC.HCl, NHS, DMF, rt, 16 h, 82%.

Compound 1a

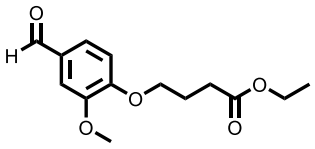

$C_{14}H_{18}O_5$
266.2930 g mol^{-1}

4.4 mL ethyl-4-bromobutyrate (6.00 g, 30.8 mmol, 1.00 equiv.) and 4.68 g vanillin (30.8 mmol, 1.00 equiv.) were dissolved in 50 mL DMF. 6.81 g K_2CO_3 (49.3 mmol, 1.60 equiv.) was added and the mixture heated to 50 °C under stirring for 2 h. Subsequently, the mixture was filtered, diluted with 50 mL water and extracted with 100 mL ethyl acetate. The organic extract was twice washed with 100 mL water, 100 mL brine, dried over Na_2SO_4 and concentrated in vacuo to give 6.72 g product (82%, 25.2 mmol) as a white solid.

R_f (DCM) = 0.63 – The product was stained using $KMnO_4$-solution.

^{1}H-NMR (400 MHz, $CDCl_3$): δ (ppm) = 9.84 (s, 1H, C*H*O), 7.42 (dd, *J* = 8.2, 1.7 Hz, 1H, Ar-*H*), 7.40 (d, *J* = 1.7 Hz, 1H, Ar-*H*), 6.98 (d, *J* = 8.2 Hz, 1H, Ar-*H*), 4.15 (t, *J* = 7.2 Hz, 2H, OC*H*$_2$CH$_2$CH$_2$CO), 4.12 (d, *J* = 7.2 Hz, 2H, OC*H*$_2$CH$_3$), 3.92 (s, 3H, OC*H*$_3$), 2.54 (t, *J* = 7.2 Hz, 2H, OCH$_2$CH$_2$C*H*$_2$CO), 2.19 (p, *J* = 7.2 Hz, 2H, OCH$_2$C*H*$_2$CH$_2$CO), 1.26 (t, *J* = 7.2 Hz, 3H, OCH$_2$C*H*$_3$).

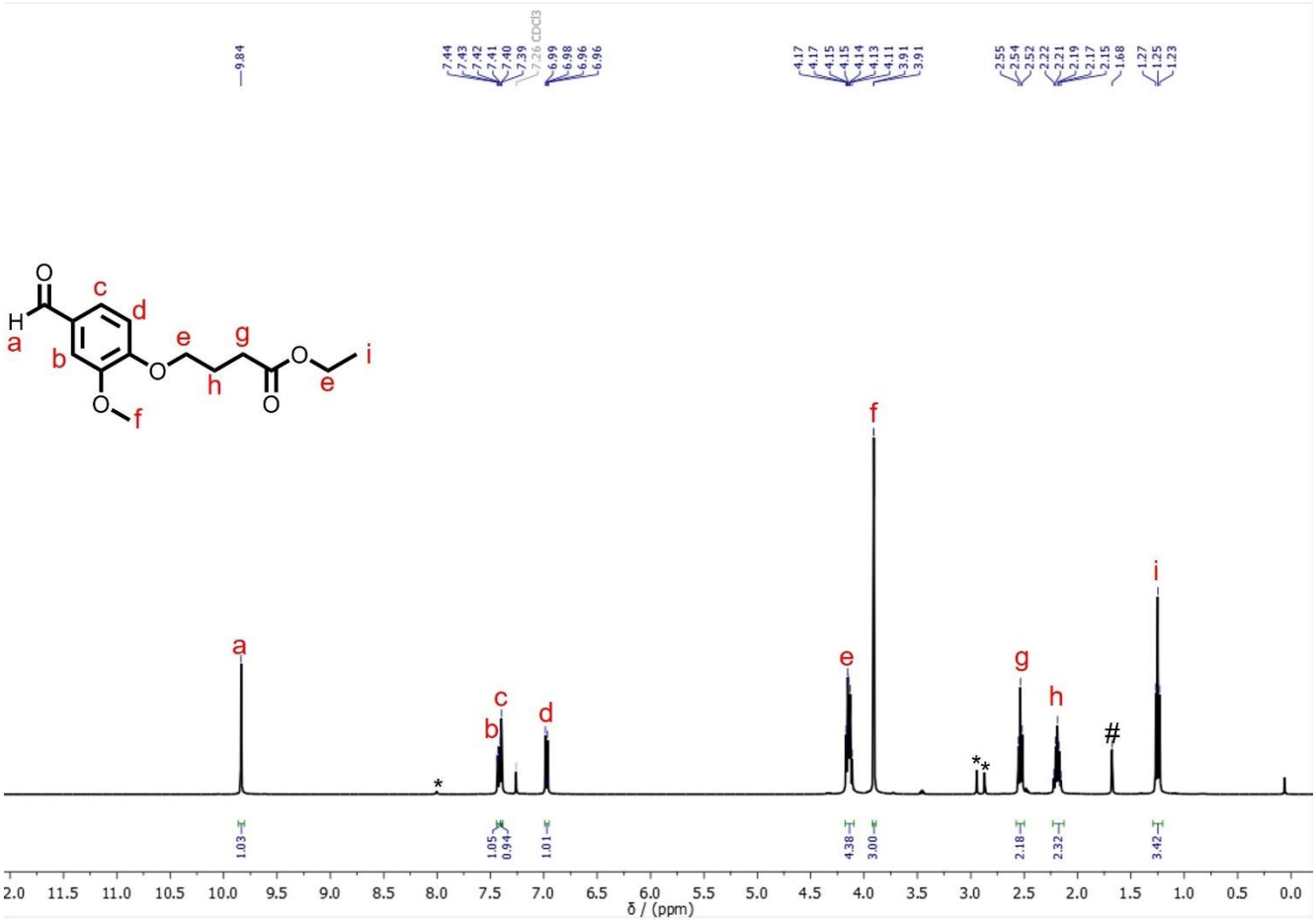

Figure S2: ^{1}H NMR spectrum of compound **1a** ($CDCl_3$, 400 MHz, #: water, *: DMF).

The spectroscopic data is in agreement with literature.[1]

Compound 1b

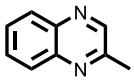

$C_9H_8N_2$
144.1770 g mol^{-1}

4.62 mL methylglyoxal (40% in H_2O, 5.40 g, 74.9 mmol, 2.00 equiv.) was added to a solution of 4.05 g benzene-1,2-diamine (37.5 mmol, 1.00 equiv.) and 1.20 g ZnI_2 (3.75 mmol, 0.10 equiv.) in 40 mL ethanol/water (1:1 v/v) and the solution was heated at 80 °C for 1 h. The solution was then partially concentrated in vacuo, 2x extracted with 50 mL CH_2Cl_2, dried over Na_2SO_4 and concentrated in vacuo. The crude product was purified by column chromatography (*n*-Hex / EtOAc 7:3) to give 3.30 g product (61%, 22.9 mmol) as a yellow liquid.

R_f (*n*-Hex / EtOAc 7:3) = 0.41.

^{1}H-NMR (400 MHz, $CDCl_3$): δ (ppm) = 8.74 (s, 1H, N-C*H*), 8.07-8.02 (m, 2H, 2x C*H*-Ar), 7.76-7.67 (m, 2H, 2x C*H*-Ar), 2.77 (s, 3H, CH_3).

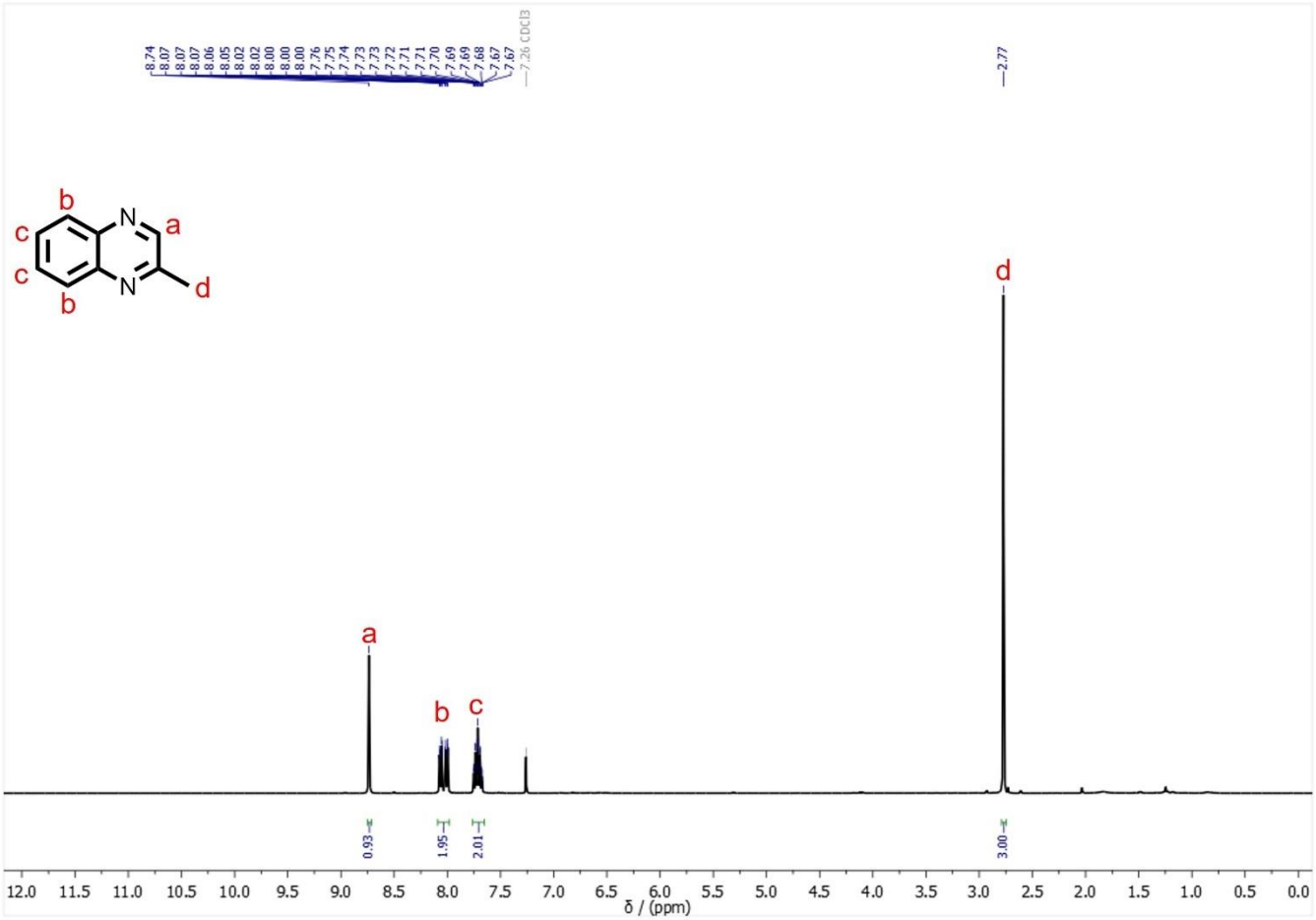

Figure S3: ^{1}H NMR spectrum of compound **1b** ($CDCl_3$, 400 MHz).

The spectroscopic data is in agreement with literature.[2]

Compound 1c

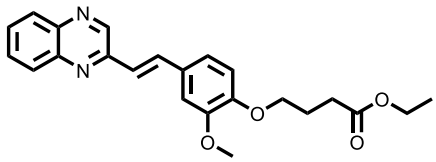

$C_{23}H_{24}N_2O_4$
392.4550 g mol^{-1}

To a mixture of 3.26 g **1a** (12.2 mmol, 1.00 equiv.) and 2.11 g **1b** (14.6 mmol, 1.20 equiv.) was added 604 µL piperidine (519 mg, 6.10 mmol, 0.50 equiv.), 523 µL acetic acid (550 mg, 9.15 mmol, 0.75 equiv.) and 5 mL dry toluene. The mixture was purged with argon, sealed and heated at 115 °C for 48 h. The resultant solution was concentrated in vacuo and absorbed onto silica gel. Column chromatography (*n*-Hex / EtOAc 2:1) delivered 3.40 g product (71%, 8.66 mmol) as yellow solid.

R_f (*n*-Hex / EtOAc 2:1) = 0.38.

^{1}H-NMR (400 MHz, $CDCl_3$): δ (ppm) = 9.09 (s, 1H, N-*H*), 8.09 (td, *J* = 7.9, 7.3, 1.6 Hz, 2H, Ar-*H*), 7.85 (d, *J* = 16.4 Hz, 1H, Ar-*H*-OCH_3), 7.78-7.71 (m, 2H, Ar-*H*), 7.31 (d, *J* = 5.0 Hz, 1H, C*H*), 7.28 – 7.18 (m, 2H, Ar-*H*), 6.96(d, *J* = 8.3 Hz, 1H, C*H*), 4.22-4.15 (m, 4H, 2x CH_2), 3.98 (s, 3H, OCH_3), 2.59 (t, *J* = 7.2 Hz, 2H, CH_2), 2.23 (p, J = 7.2 Hz, 2H, CH_2), 1.30 (t, *J* = 7.2 Hz, 3H, CH_3).

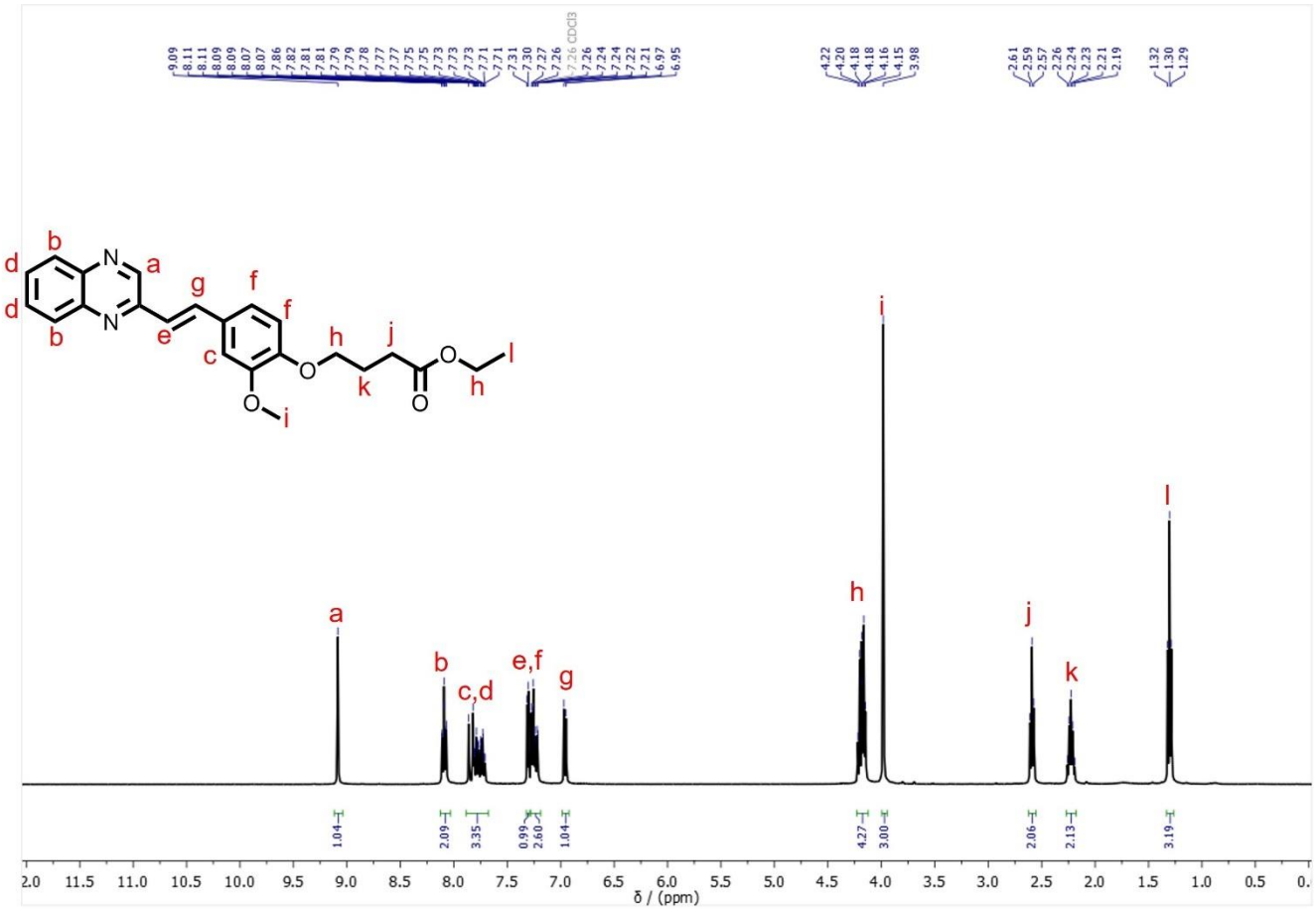

Figure S4: ^{1}H NMR spectrum of compound **1c** ($CDCl_3$, 400 MHz).

The spectroscopic data is in agreement with literature.[2]

Compound 1d

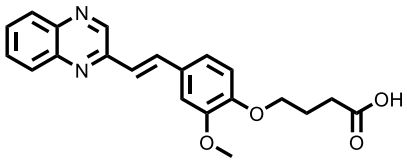

$C_{21}H_{20}N_2O_4$
364.4010 g mol^{-1}

716 mg **1c** (1.82 mmol, 1.00 equiv.) was dissolved in 10 mL THF. To this solution was added a suspension of 87.4 mg LiOH (3.65 mmol, 2.00 equiv.) in 10 mL water and the solution was stirred at ambient temperature for 1 h. The solution was partially concentrated in vacuo and pH was adjusted to 6 using 3 mL 1M HCl solution. The solution was further diluted with 100 mL water, filtered, and dried in vacuo to give 536 mg (81%, 1.47 mmol) product as yellow solid.

^{1}H-NMR (400 MHz, DMSO-d_6): δ (ppm) = 12.18 (bs, 1H, O*H*), 9.21 (s, 1H, N-*H*), 8.03 (t, *J* = 9.2 Hz, 2H, Ar-*H*), 7.95 (d, *J* = 16.3 Hz, 1H, Ar-*H*-OCH$_3$), 7.80 (dt, *J* = 24.8, 7.3 Hz, 2H, Ar-*H*), 7.48 (d, *J* = 16.3 Hz, 1H, C*H*), 7.27 (dd, *J* = 8.3, 1.9 Hz, 1H, Ar-*H*), 7.02 (d, *J* = 8.3 Hz, 1H, C*H*), 4.03 (t, *J* = 6.4 Hz, 2H, CH_2), 3.87 (s, 3H, OCH_3), 2.40 (t, *J* = 7.3 Hz, 2H, CH_2), 1.96 (p, *J* = 6.9 Hz, 2H, CH_2).

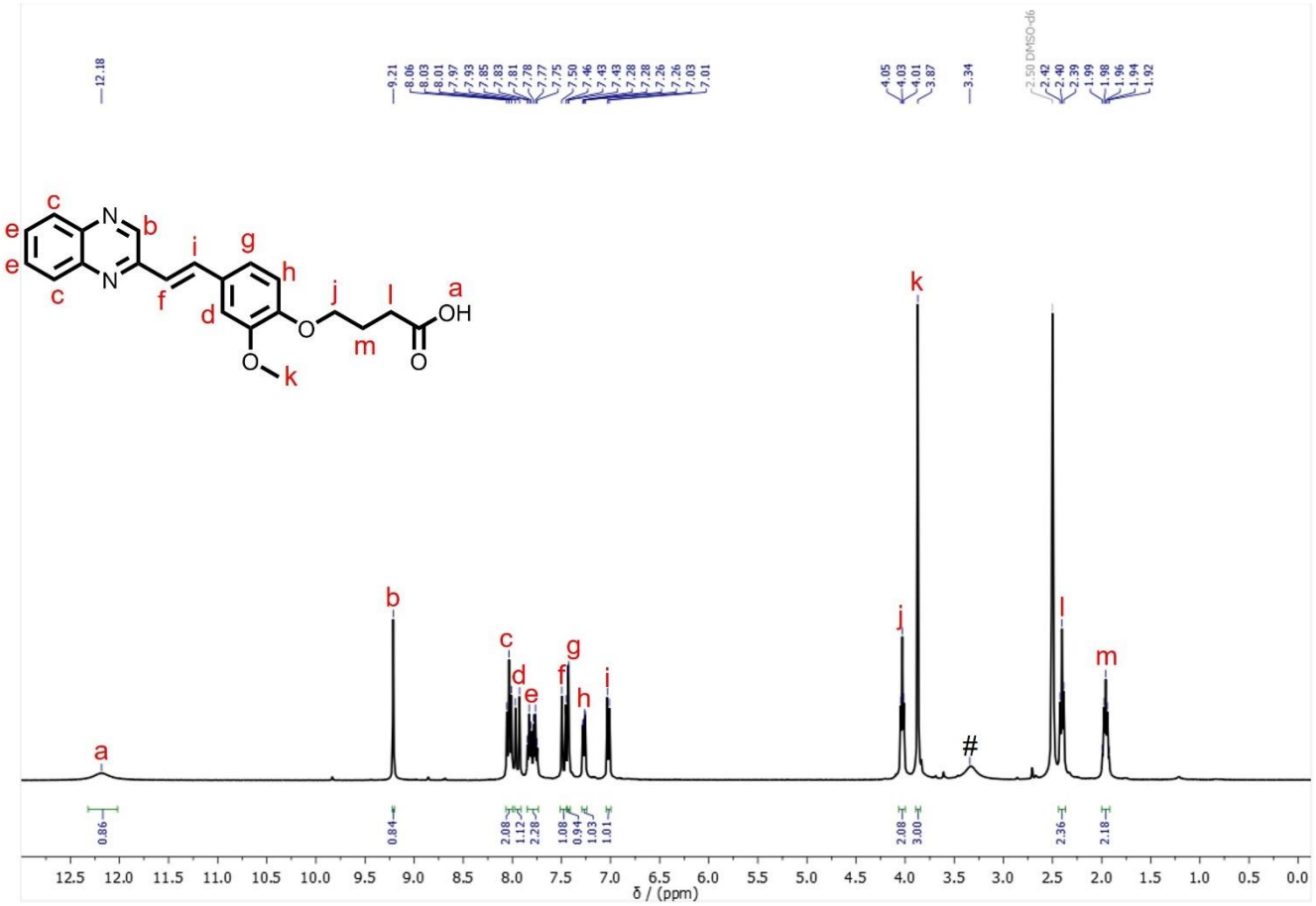

Figure S5: ^{1}H NMR spectrum of compound **1d** (DMSO-d_6, 400 MHz, #: water).

The spectroscopic data is in agreement with literature.[2]

Compound 1

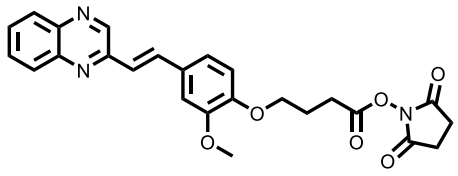

$C_{25}H_{23}N_3O_6$
461.47 g mol^{-1}

200 mg **1d** (549 µmol, 1.00 equiv.) was dissolved in 5 mL DMF. To this solution, 158 mg N-(3-dimethylaminopropyl)-N'-ethylcarbodiimide hydrochloride (EDC.HCl, 824 µmol, 1.50 equiv.) and 94.8 mg N-hydroxysuccinimide (824 µmol, 1.50 equiv.) were added and the solution was stirred at ambient temperature for 6 h. DMF was concentrated in vacuo and the residue was absorbed onto silica gel (ca. 500 mg). Column chromatography (*n*-Hex / EtOAc = 3:7) delivered 208 mg SQ-NHS ester **1** (82%, 450 µmol) as a yellow solid.

R_f (*n*-Hex / EtOAc 3:7) = 0.48.

^{1}H-NMR (400 MHz, $CDCl_3$): δ (ppm) = 9.06 (s, 1H, N-*H*), 8.06 (ddd, *J* = 8.2, 3.1, 1.5 Hz, 2H, Ar-*H*), 7.81 (d, *J* = 16.3 Hz, 1H, Ar-*H*-OCH_3), 7.73 (dddd, *J* = 23.7, 8.3 6.9, 1.5 Hz, 2H, Ar-*H*), 7.30 – 7.25 (m, 1H, C*H*), 7.23 – 7.18 (m, 2H, Ar-*H*), 6.94 (d, *J* = 8.2 Hz, 1H, C*H*), 4.17 (t, *J* = 6.1 Hz, 2H, CH_2), 3.95 (s, 3H, OCH_3), 2.91 (t, *J* = 7.3 Hz, 2H, CH_2), 2.84 (bs, 4H, 2x CH_2), 2.29 (t, *J* = 6.7 Hz, 2H, CH_2).

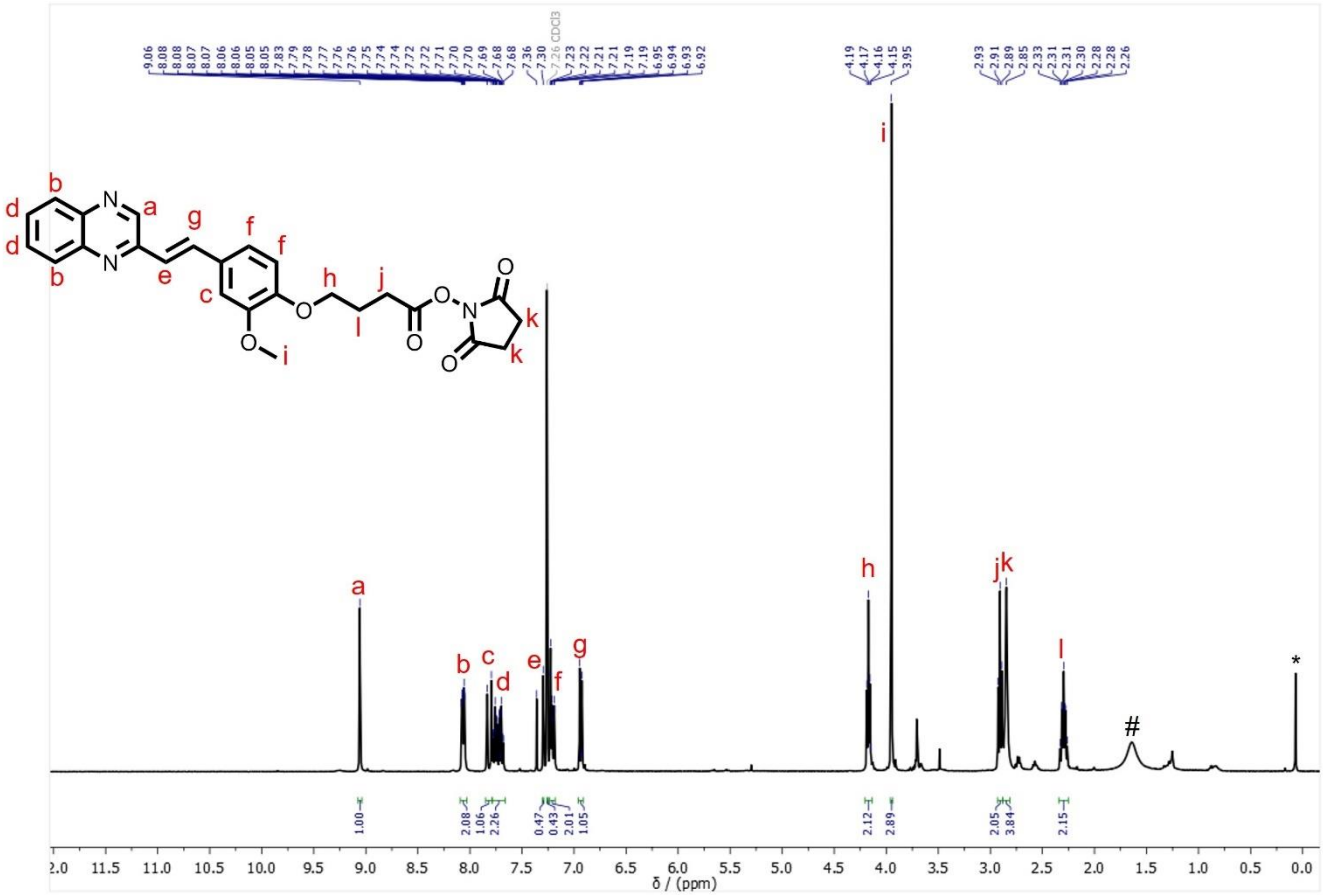

Figure S6: ^{1}H NMR spectrum of compound **1** ($CDCl_3$, 400 MHz, #: water, *: silicon grease).

The spectroscopic data is in agreement with literature.[2]

2.2 Synthesis of Compound 2

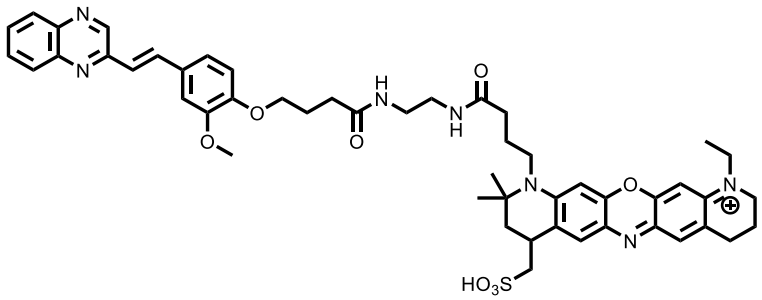

$C_{50}H_{58}N_7O_8S^+$
917.11 g mol^{-1}

5.00 mg Atto655-NH_2 (8.76 µmol, 1.00 equiv.) and 6 µL DIPEA (4.53 mg, 35.0 µmol, 4.00 equiv.) was dissolved in 2 mL anhydrous DMF. To this solution was slowly added a solution of 7.85 mg **1** (17.0 mmol, 1.00 equiv.) in 2 mL anhydrous DMF. The reaction mixture was stirred for 16 h at ambient temperature, followed by removal of the solvent under reduced pressure. The crude product was lyophilized from benzene / MeOH (5:4) solution, affording 5.54 mg SQ-modified Atto655 dye **2** (69%, 6.04 µmol) as a blue-green solid.

R_f (DCM / MeOH 10:1) = 0.45.

The resulting product was characterized via ESI-HRMS.

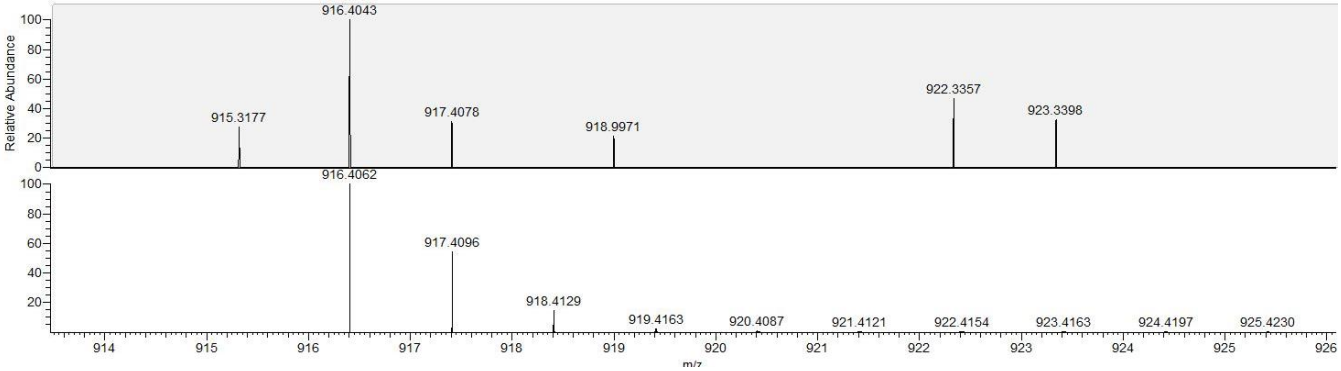

Figure S7: ESI-HRMS analysis of **2**: $M_{calc.}$ = 916.4062 g mol^{-1} [$C_{50}H_{58}N_7O_8S^-$], $M_{meas.}$ = 916.4043 g mol^{-1} [$C_{50}H_{58}N_7O_8S^-$].

2.3 Synthesis of Compound 3 and 4

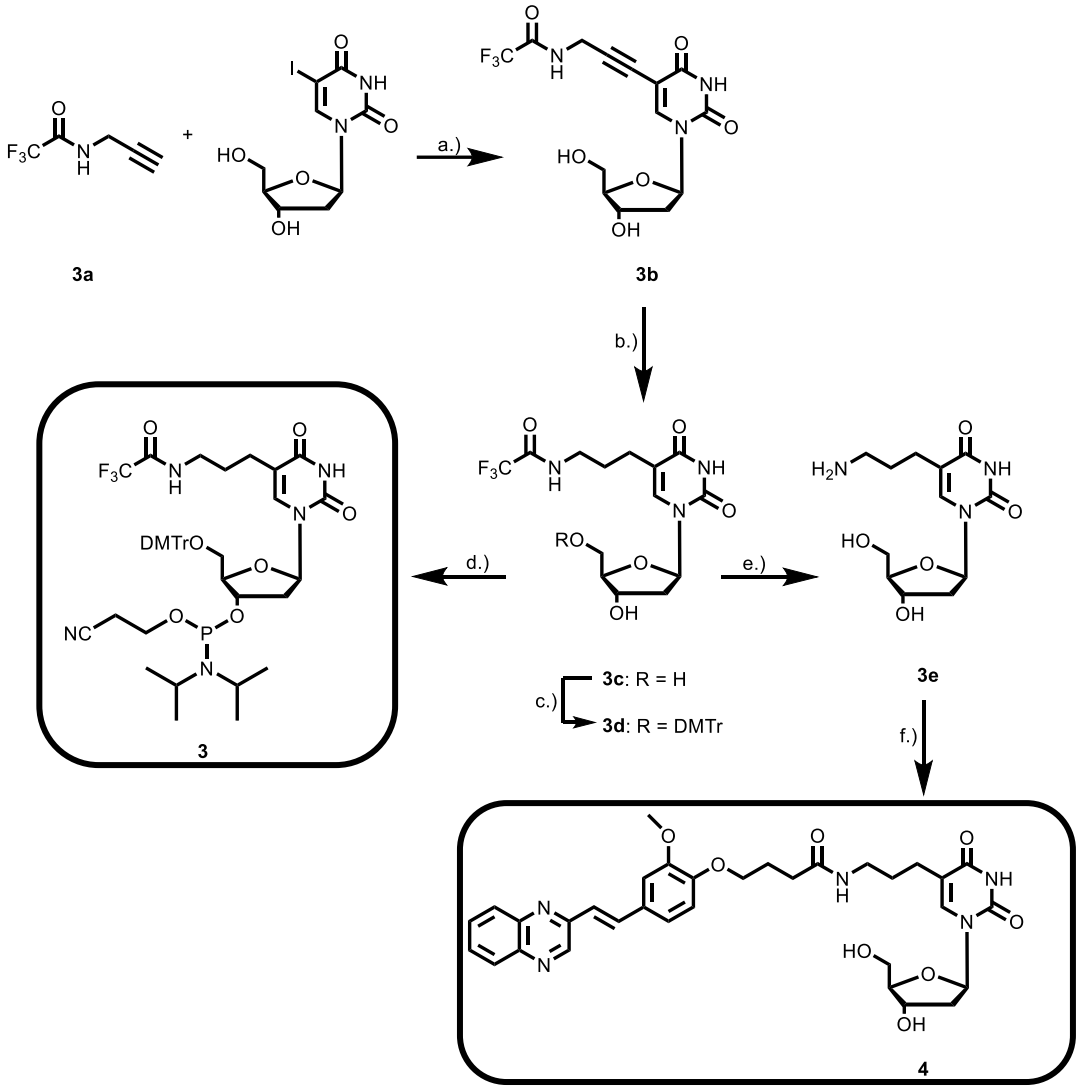

Scheme S2: Synthesis of the aminopropyl-modified phosphoramidite building block **3**: a.) Copper(I) iodide, tetrakis(triphenylphosphine)palladium(0), triethylamine, DMF, 50°C, 5 h, 55%; b.) Hydrogen, Pd/C, MeOH, r.t., 6 h, 80%; c.) 4,4'-dimethodytrityl chloride, silver(II) nitrate, pyridine, r.t., 16 h, 60%; d.) 2-Cyanoethyl N,N-diisopropyl-chlorophosphoramidite, DIPEA, DCM, r.t., 2 h, 63%; e.) conc. NH_4OH, r.t., 16 h, 77%; f.) Synthesis of SQ-modified nucleoside **4**: **1**, DIPEA, DMF, r.t., 16h, 43%.

Compound 3a

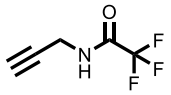

$C_5H_4F_3NO$
151.09 g mol^{-1}

4.50 mL ethyl trifluoroacetate (5.33 g, 38.0 mmol, 1.20 equiv.) were slowly added to an ice-cold solution of 2.00 mL propargylamine (1.72 g, 31.00 mmol, 1.00 equiv.) in 30 mL MeOH. After stirring for 24 h at ambient temperature, the solvent was removed under reduced pressure, followed by diluting the residue in 50 mL DCM. Saturated $NaHCO_3$ solution was added to the residue and the aqueous phase was extracted 3x with 100 mL DCM. The combined organic layers were dried over sodium sulfate, filtered and the solvent was removed under reduced pressure. Column chromatography (DCM) delivered 2.84 g (60%, 18.8 mmol) of the amide as yellow liquid.

R_f (DCM) = 0.80 – The product was visualized using $KMnO_4$-solution.

^{1}H-NMR (400 MHz, $CDCl_3$): δ (ppm) = 6.57 (bs, 1H, N*H*), 4.16 (dd, *J* = 5.5, 2.5 Hz, 2H, CH_2), 2.33 (t, *J* = 2.6 Hz, 1H, C*H*).

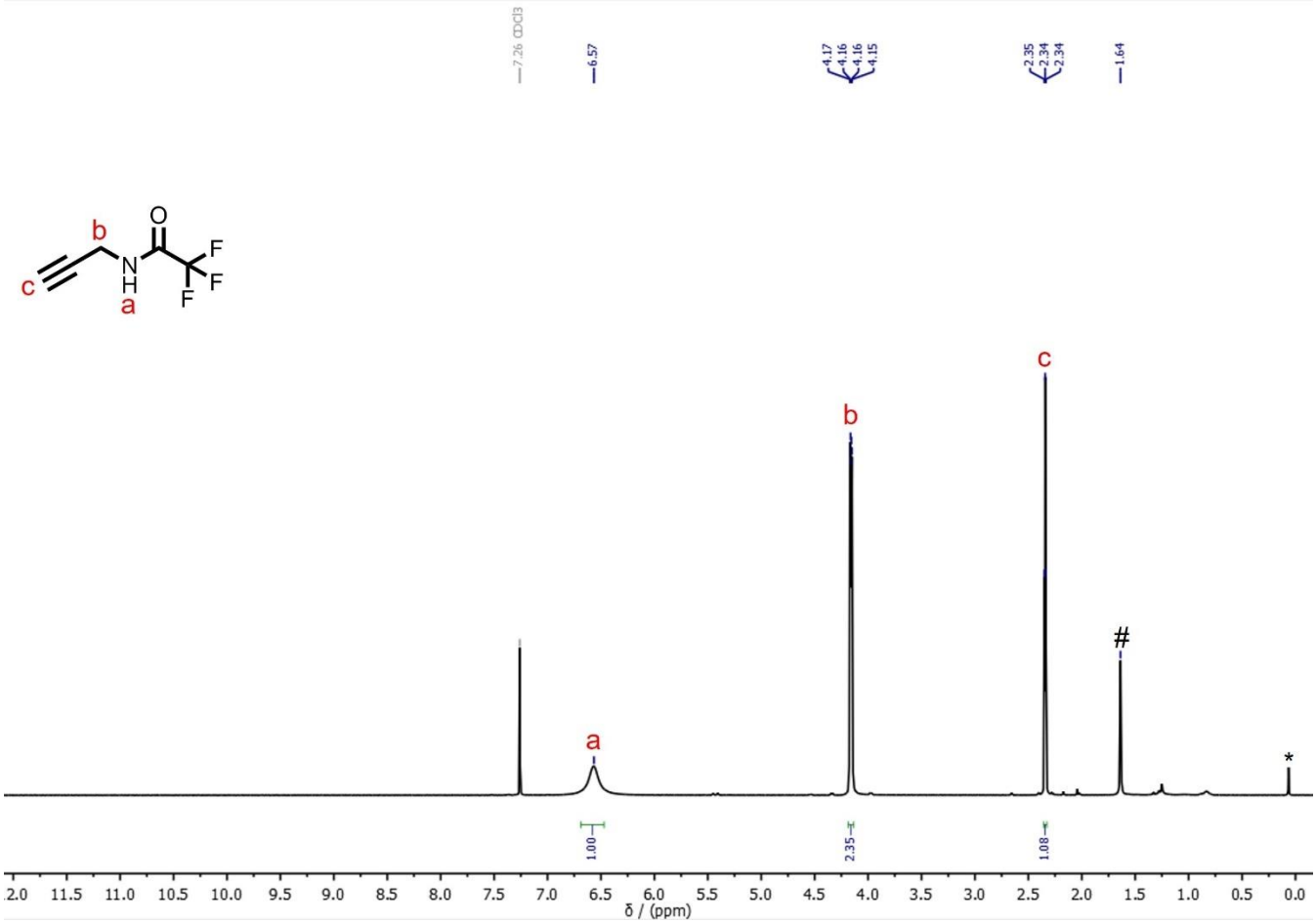

Figure S8: ^{1}H NMR spectrum of compound **3a** ($CDCl_3$, 400 MHz, #: water, *: silicon grease).

The spectroscopic data is in agreement with literature.[3]

Compound 3b

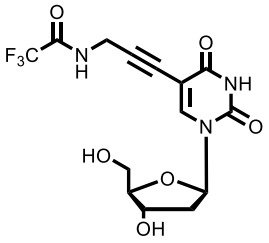

$C_{14}H_{14}F_3N_3O_6$
377.28 g mol^{-1}

Under an argon atmosphere, 2.33 g 5-iodo-2'-deoxyuridine (6.60 mmol, 1.00 equiv.) was dissolved in 25 mL anhydrous DMF. 251 mg copper(I) iodide (1.32 mmol, 0.20 equiv.) and 2.20 µL **3a** (2.84 g, 19.8 mmol, 3.00 equiv.) were added. The reaction was degassed by bubbling with argon gas for 15 min. 763 mg tetrakis(triphenyl-phosphine)palladium(0) (660 µmol, 0.10 equiv.) and 1.82 mL triethylamine (1.34 mg, 13.2 mmol, 2.00 equiv.) were added and the reaction stirred for 16 h at ambient temperature. The solvent was removed under reduced pressure and the crude product dissolved in 100 mL MeOH/DCM 1:1 (v/v). Two teaspoons of freshly prepared AMBERLITE® *IRA-402* (bicarbonate form) were added and the resulting suspension stirred for 15 min. After filtration, the solvent was removed under reduced pressure and the crude product purified via column chromatography (DCM/MeOH 10:1). The product was obtained as a brown foam (1.37 g, 55%, 3.63 mmol).

R_f (DCM/MeOH 10:1) = 0.23 – The product was stained using 5% H_2SO_4 solution.

^{1}H-NMR (400 MHz, DMSO-d_6): δ (ppm) = 11.63 (s, 1H, 3-N*H*), 10.06 (d, *J* = 5.6 Hz, 1H, N*H*), 8.19 (s, 1H, 6-C*H*), 6.10 (t, *J* = 6.7 Hz, 1H, 1'-C*H*), 5.23 (d, *J* = 4.3 Hz, 1H, 3'-O*H*), 5.08 (t, *J* = 5.1 Hz, 1H, 5'-O*H*), 4.23 (d, *J* = 4.7 Hz, 3H, 3'-CH, CH_2), 3.79 (q, *J* = 3.4 Hz, 1H, 4'-C*H*), 3.58 (ddd, *J* = 10.5, 5.1, 3.5 Hz, 2H, 5'-CH_2), 2.13 - 2.10 (m, 2H, 2'-CH_2).

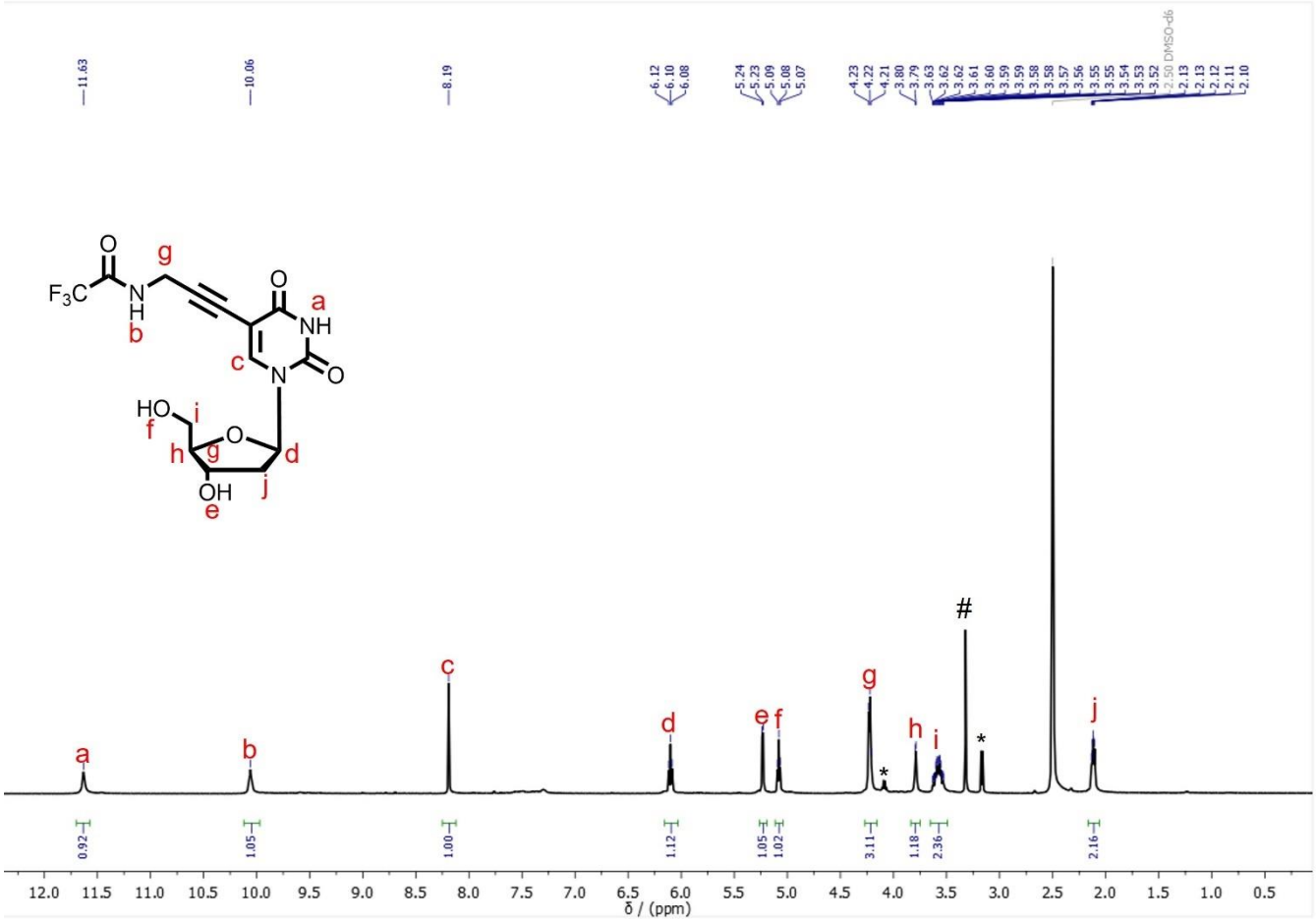

Figure S9: ^{1}H NMR spectrum of compound **3b** (DMSO-d_6, 400 MHz, #: water, *: MeOH).

The spectroscopic data is in agreement with literature.[4]

Compound 3c

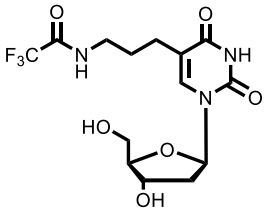

$C_{14}H_{18}F_3N_3O_6$
381.31 g mol^{-1}

730 mg nucleoside **3b** (1.93 mmol, 1.00 equiv.) and 309 mg Pd/C (10% Pd, 290 µmol, 0.15 equiv.) were dissolved in 25 mL anhydrous MeOH. Hydrogen (approx. 3 L balloon) was bubbled through the suspension for 5 h. The reaction mixture was filtered over a plug of CELITE®, followed by removal of the solvent under reduced pressure. 589 mg (80%, 1.54 mmol) of the product were obtained as a light brown foam.

R_f (DCM/MeOH 10:1) = 0.18 – The product was stained using 5% H_2SO_4 solution.

^{1}H-NMR (400 MHz, DMSO-d_6): δ (ppm) = 11.29 (s, 1H, 3-N*H*), 9.40 (t, *J* = 5.2 Hz, 1H, N*H*), 7.68 (s, 1H, 6-C*H*), 6.16 (t, *J* = 6.8, 1H, 1'-C*H*), 5.22 (d, *J* = 4.2 Hz, 1H, 3'-O*H*), 5.00 (t, *J* = 5.2 Hz, 1H, 5'-O*H*), 4.23 (td, *J* = 6.1, 5.2, 3.1 Hz, 1H, 3'-C*H*), 3.76 (q, *J* = 3.7 Hz, 1H, 4'-C*H*), 3.56 (pt, *J* = 9.1, 4.9 Hz, 2H, 5'-CH_2), 3.17 (dd, *J* = 5.6, 2.7 Hz, 2H, CH_2), 2.20 (q, *J* = 7.2 Hz, 2H, CH_2), 2.10 – 2.07 (m, 2H, 2'-CH_2), 1.64 (qd, *J* = 7.2, 2.0 Hz, 2H, CH_2).

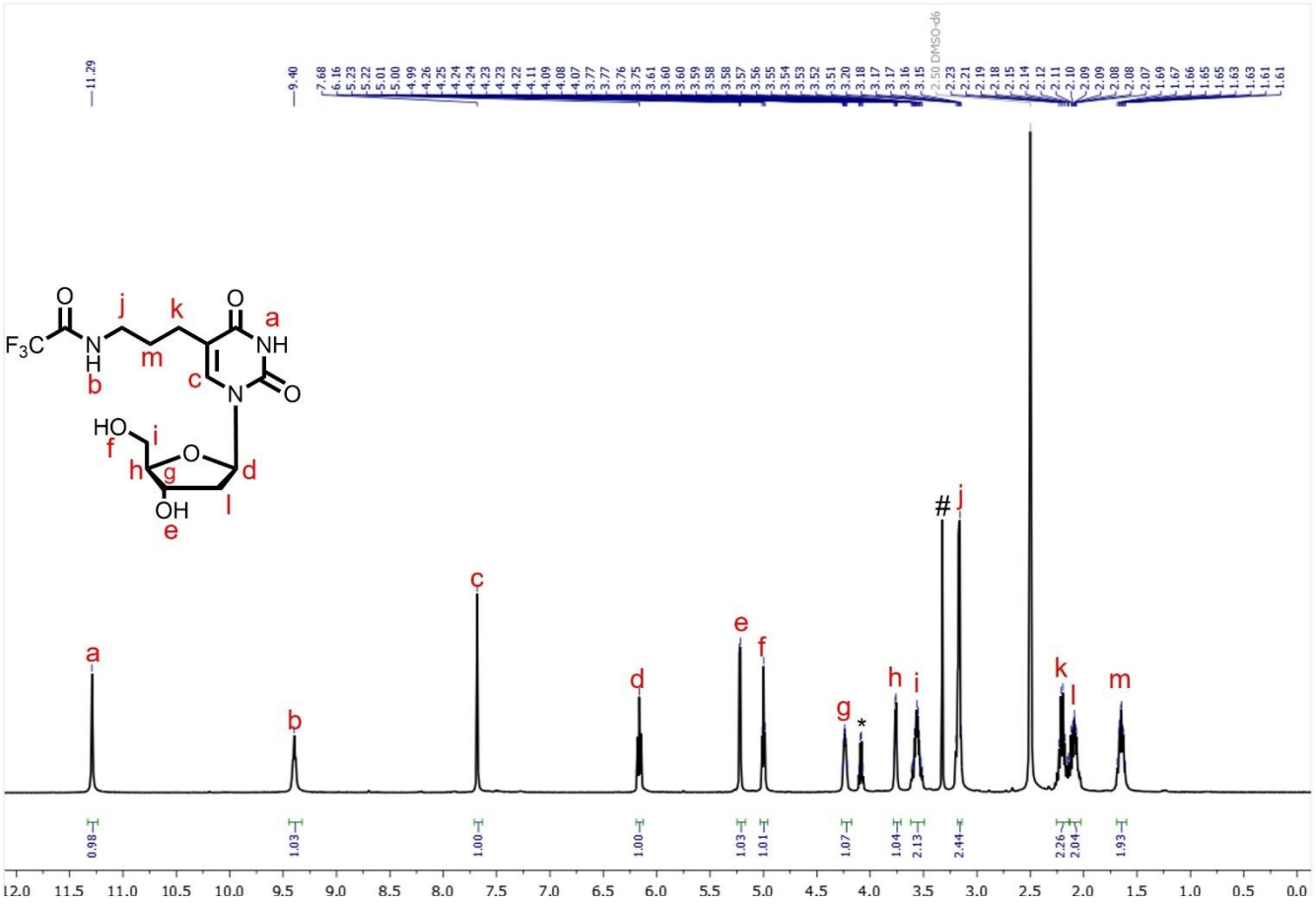

Figure S10: ^{1}H NMR spectrum of compound **3c** (DMSO-d_6, 400 MHz, #: water, *: ethyl acetate).

The spectroscopic data is in agreement with literature.[5]

Compound 3d

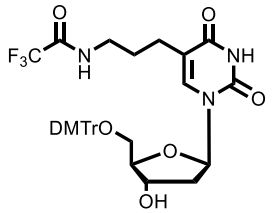

$C_{35}H_{36}F_3N_3O_8$
683.68 g mol^{-1}

Under an argon atmosphere, 600 mg **3c** (1.58 mmol, 1.00 equiv.) were dissolved in 12.0 mL anhydrous pyridine. 322 mg silver(II) nitrate (1.90 mmol, 1.20 equiv.) and 644 mg 4,4'-dimethoxytrityl chloride (1.57 mmol, 1.20 equiv.) were added and the reaction mixture stirred for 6 h. The crude mixture was diluted with 50 mL DCM, filtered and washed 3x with 50 mL saturated $NaHCO_3$ solution. The solvent was removed under reduced pressure. Column chromatography (DCM/MeOH 40:1 to 20:1) and following lyophilization from benzene delivered 648 mg (60%, 948 µmol) of a brown/beige foam.

R_f (DCM/MeOH 10:1) = 0.65 – The product was stained using 5% H_2SO_4 solution.

^{1}H-NMR (400 MHz, DMSO-d_6): δ (ppm) = 11.37 (s, 1H, 3-N*H*), 9.34 (t, *J* = 5.5 Hz, 1H, N*H*), 7.41 (s, 1H, 6-C*H*), 7.39 – 7.37 (m, 2H, CH_{ar}), 7.32 – 7.22 (m, 7H, CH_{ar}), 6.88 (dd, 4H, *J* = 8.9, 1.7 Hz, CH_{ar}), 6.19 (t, *J* = 6.8 Hz, 1H, 1'-C*H*), 5.32 (d, *J* = 4.6 Hz, 1H, 3'-O*H*), 4.29 (dq, *J* = 8.2, 4.1 Hz, 1H, 3'-C*H*), 3.87 (q, *J* = 4.0 Hz, 1H, 4'-C*H*), 3.73 (s, 6H, 2x OCH_3), 3.18 (ddt, *J* = 13.4, 10.4, 4.1 Hz, 2H, 5'-CH_2), 2.97 (q, *J* = 6.8 Hz, 2H, CH_2), 2.26 (dt, *J* = 13.6, 6.9 Hz, 1H, 2'-CH_2), 2.15 (ddd, *J* = 13.4, 6.6, 3.8 Hz, 1H, 2'-CH_2), 1.91 (q, *J* = 6.7 Hz, 2H, CH_2), 1.47 (dq, J = 14.3, 6.5 Hz, 2H, CH_2).

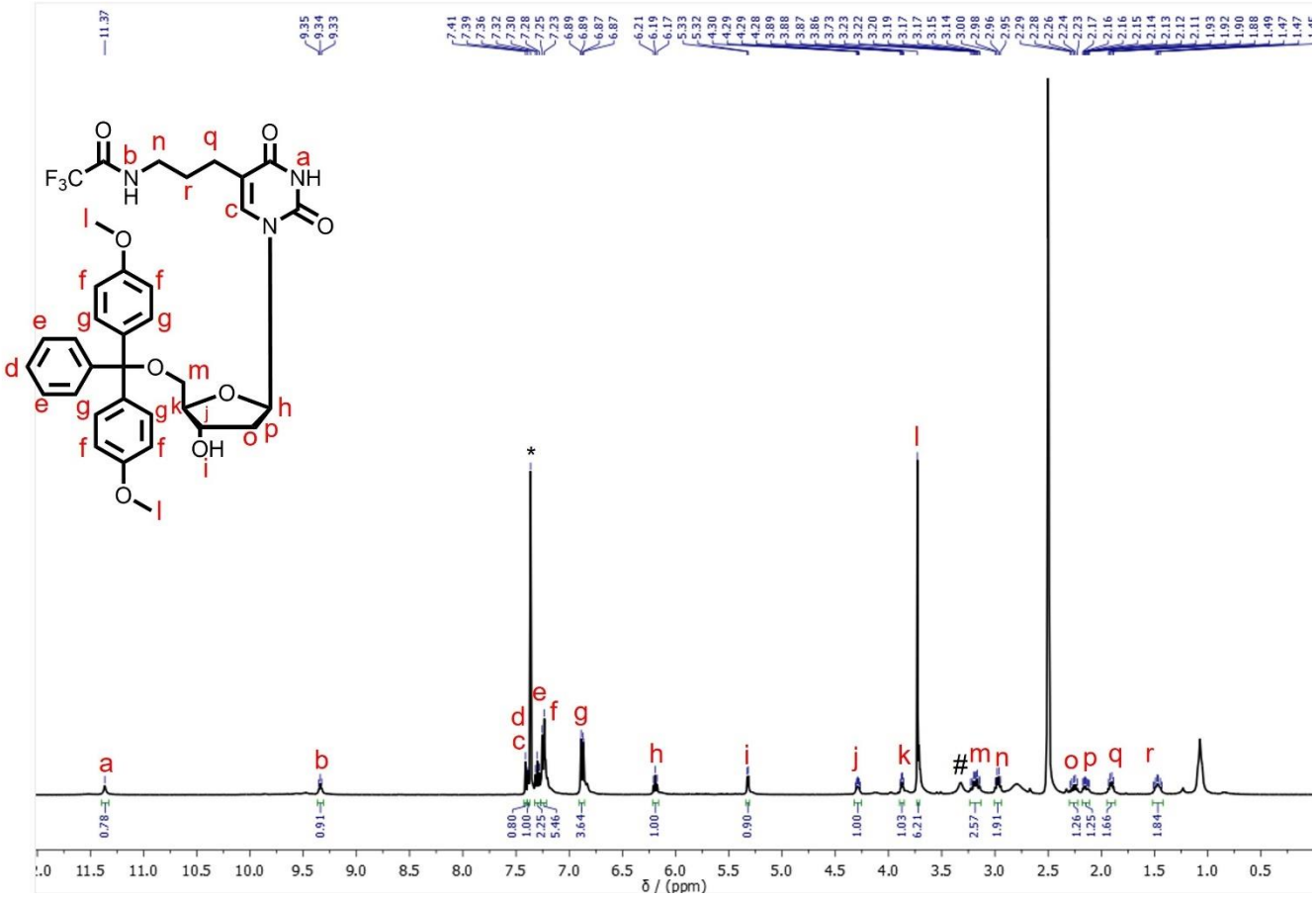

Figure S11: ^{1}H NMR spectrum of compound **3d** (DMSO-d_6, 400 MHz, #: water, *: benzene).

The spectroscopic data is in agreement with literature.[6]

Compound 3

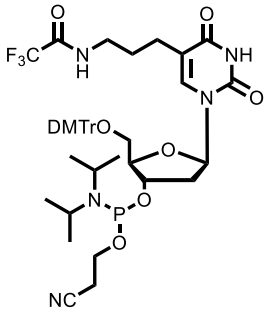

$C_{44}H_{53}F_3N_5O_9P$
883.9030 g mol^{-1}

75.0 mg **3d** (110 µmol, 1.00 equiv.) were lyophilized from 5 mL benzene and dissolved in 3 mL anhydrous DCM. 56 µL DIPEA (42.5 mg, 329 µmol, 3.00 equiv.) and 37 µL 2-cyano-ethyl-N-N-diisopropylchlorophosphoramidite (39.1 mg, 165 µmol, 1.50 equiv.) were added and the reaction mixture stirred for 4 h. The crude product was purified via column chromatography (DCM/Acetone 3:1), yielding 61.3 mg product (63%, 69.3 µmol) as light beige foam.

R_f (DCM/Acetone 3:1) = 0.73 – The product was stained using 5% H_2SO_4 solution.

^{1}H-NMR (400 MHz, DMSO-d_6): δ (ppm) = 11.38z (s, 1H, 3-N*H*), 9.34 (t, *J* = 5.5 Hz, 1H, N*H*), 7.41 (s, 1H, 6-C*H*), 7.39 – 7.37 (m, 2H, CH_{ar}), 7.32 – 7.22 (m, 7H, CH_{ar}), 6.88 (dd, 4H, *J* = 8.9, 1.7 Hz, CH_{ar}), 6.19 (t, *J* = 6.8 Hz, 1H, 1'-C*H*), 4.52 (ddt, *J* = 15.2, 10.8, 4.1 Hz, 1H, 3'-C*H*), 4.01 (dq, *J* = 20.5, 4.3 Hz, 1 H, 4'-C*H*), 3.73 (d, *J* = 2.5 Hz, 6H, 2 x OCH_3), 3.61 – 3.43 (m, 4H, 2 x CH_2), 3.24 (dt, *J* = 11.2, 2.4 Hz, 2H, 5'-CH_2), 2.99 (p, *J* = 6.6 Hz, 2H, CH_2), 2.76 (t, J = 5.9 Hz, 1H, C*H*), 2.62 (t, J = 5.9 Hz, 1H, C*H*), 2.42 – 2.24 (m, 2H, 2'-CH_2), 1.95 (dd, *J* = 16.1, 8.1 Hz, 2H, CH_2), 1.54 – 1.44 (m, 2H, CH_2)., 1.23 – 1.06 (m, 12 H, 4x CH_3).

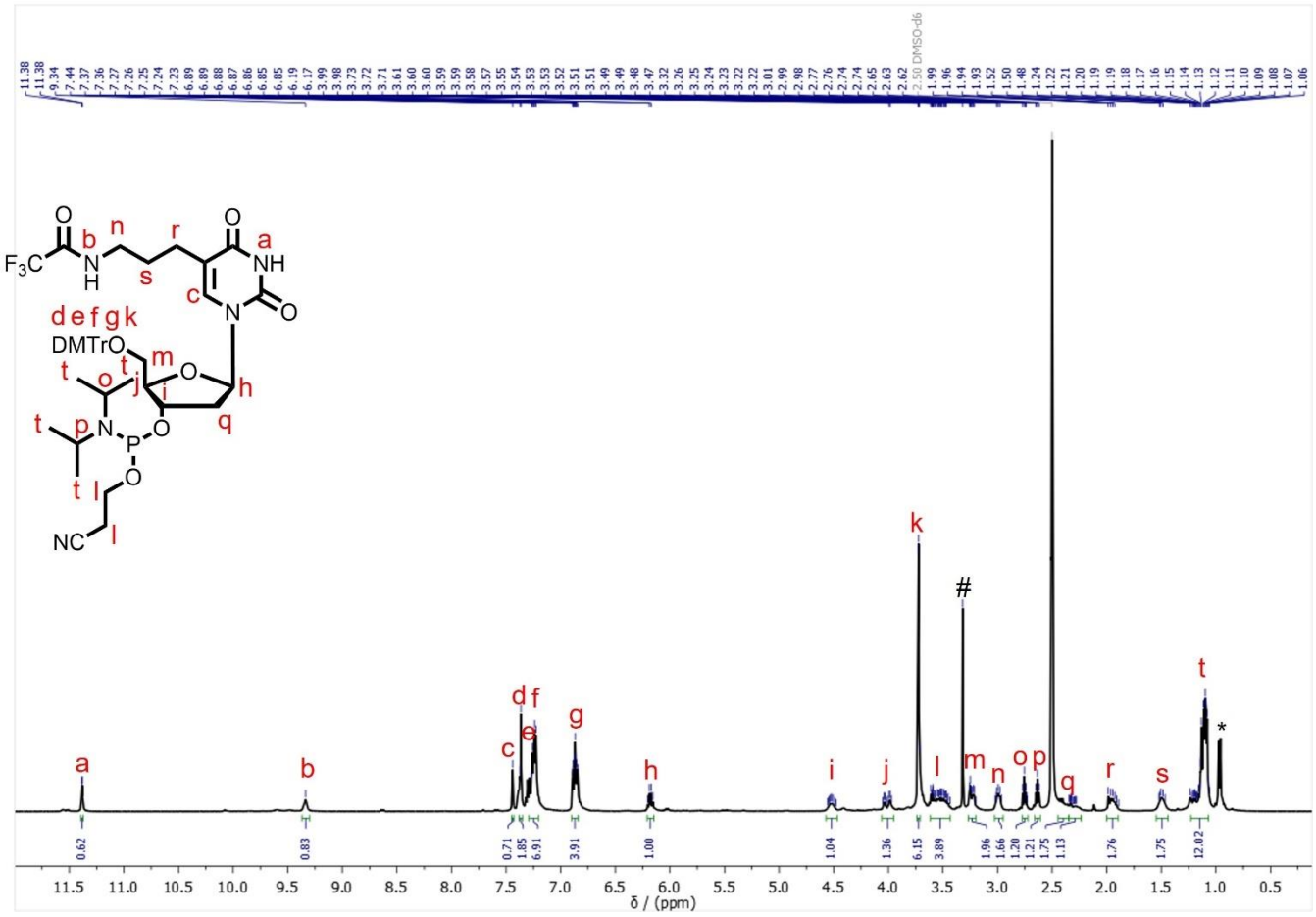

Figure S12: ^{1}H NMR spectrum of compound **3** (DMSO-d_6, 400 MHz, #: water, *: triethyl ammonium salts).

^{31}P-NMR (162 MHz, DMSO-d_6): δ (ppm) = 147.6, 147.2.

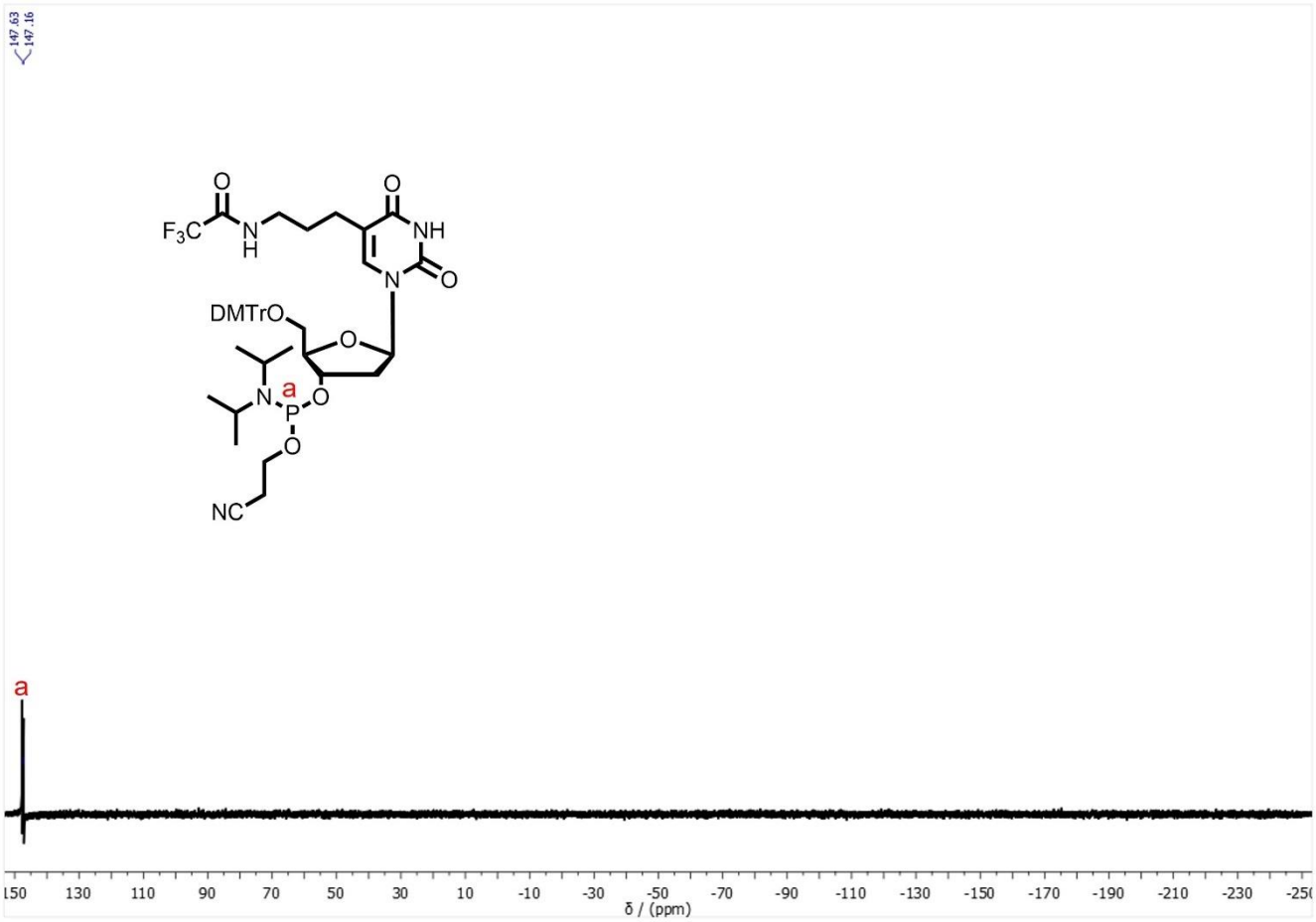

Figure S13: ^{31}P NMR spectrum of compound **3** (DMSO-d_6, 162 MHz).

The spectroscopic data is in agreement with literature.[6]

Compound 3e

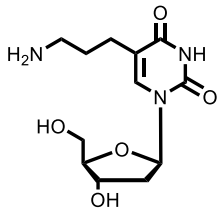

$C_{12}H_{19}N_3O_5$
285.3 g mol^{-1}

177 mg **3c** (464 µmol, 1.00 equiv.) was dissolved in 8 mL concentrated aqueous ammonia and stirred over night at ambient temperature. The solvent was removed under reduced pressure. After lyophilization from benzene, 102 mg product **3e** (77%, 357 µmol) were obtained as a brown foam.

^{1}H-NMR (400 MHz, DMSO-d_6): δ (ppm) = 11.34 (s, 1H, 3-N*H*), 7.72 (s, 3H, 6-C*H,* NH_2), 6.16 (t, *J* = 6.8 Hz, 1H, 1'-C*H*), 5.25 (d, *J* = 4.3 Hz, 1H, 3'-O*H*), 5.04 (t, *J* = 5.2 Hz, 1H, 5'-O*H*), 4.43 – 4.05 (m, 1H, 3'-C*H*), 3.78 (d, *J* = 3.4 Hz, 1H, 4'-C*H*), 3.57 (dt, *J* = 8.0, 4.2 Hz, 2H, 5'-CH_2), 2.76 (t, *J* = 7.7 Hz, 2H, CH_2), 2.26 (t, *J* = 7.4 Hz, 2H, 2'-CH_2), 2.09 (dd, J = 6.9, 4.7 Hz, 2H, CH_2), 1.71 (p, *J* = 7.5 Hz, 2H, CH_2).

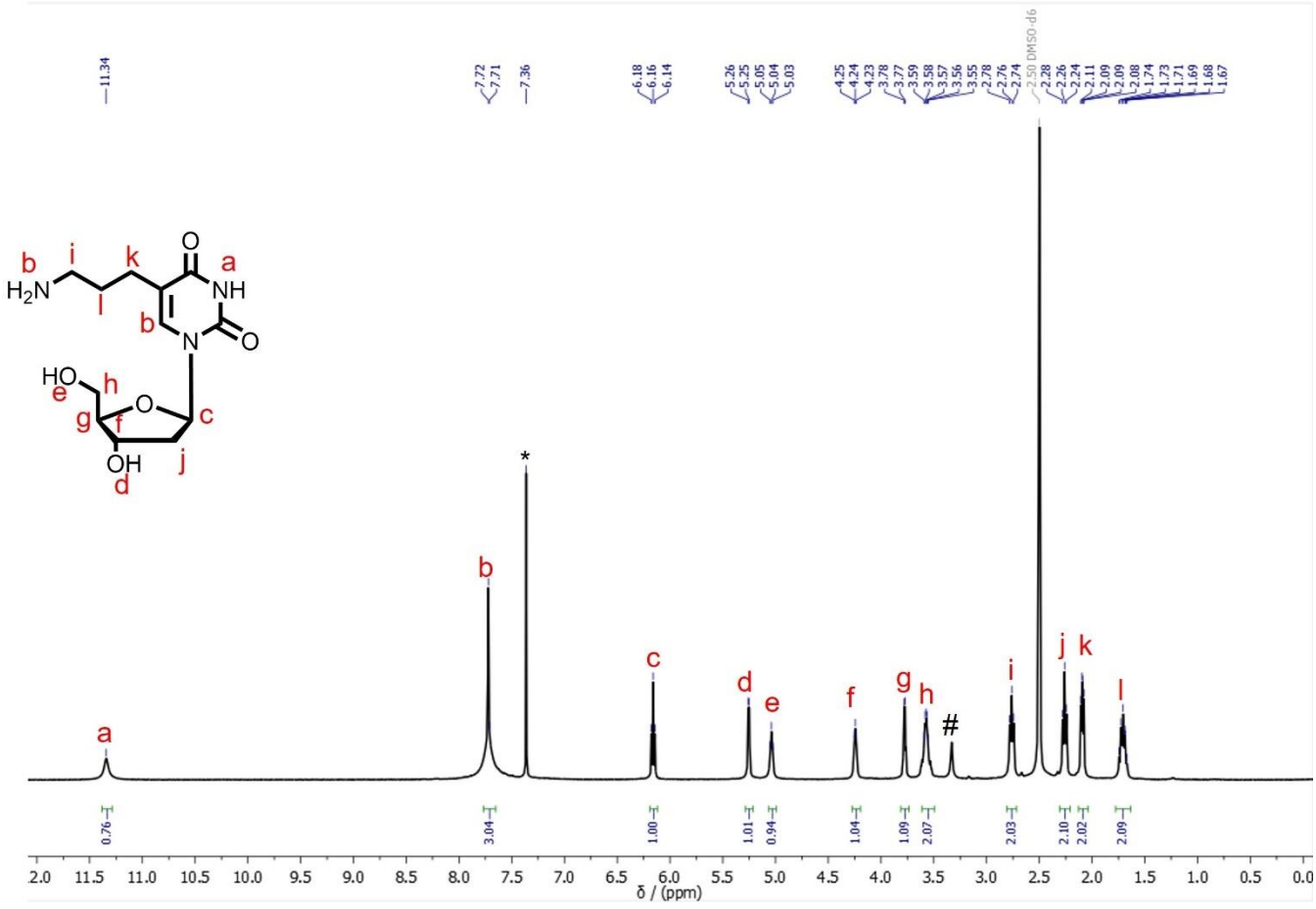

Figure S14: ^{1}H NMR spectrum of compound **3e** (DMSO-d_6, 400 MHz, #: water, *: benzene).

The spectroscopic data is in agreement with literature.[7]

Compound 4

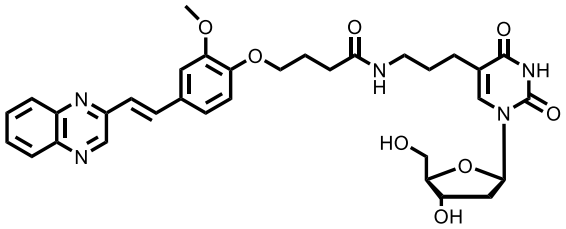

$C_{33}H_{37}N_5O_8$
631.2642 g mol^{-1}

40.0 mg **3e** (140 µmol, 1.00 equiv.) and 55 µL DIPEA (72.4 mg, 560 µmol, 4.00 equiv.) were dissolved in 3.50 mL anhydrous DMF. To this solution, a solution of 84.1 mg **1** (182 µmol, 1.30 equiv.) in 3.50 mL anhydrous DMF was slowly added, and the mixture stirred for 16 h at ambient temperature. The solvent was removed under reduced pressure, followed by purification of the crude product via column chromatography (DCM/MeOH 20:1 to 10:1). 38.2 mg product (43%, 60.2 µmol) were obtained as bright yellow powder.

R_f (DCM/MeOH 10:1) = 0.42 – The product was stained with 5% H_2SO_4 solution.

^{1}H-NMR (400 MHz, DMSO-d_6): δ (ppm) = 11.27 (s, 1H, 3-N*H*), 10.54 (bs, 1H, N*H*), 9.22 (s, 1H, N-*H*), 8.04 (ddd, *J* = 9.9, 8.1, 1.5 Hz, 2H, Ar-*H*), 7.95 (d, *J* = 16.3 Hz, 1H, C*H*), 7.88 (t, *J* = 5.7 Hz, 1H, Ar-*H*), 7.83 (ddd, *J* = 8.4, 6.9, 1.6 Hz, 1H, Ar-*H*), 7.77 (ddd, *J* = 8.3, 6.9, 1.6 Hz, 1H, Ar-*H*), 7.69 (s, 1H, 6-C*H*), 7.48 (d, *J* = 16.3 Hz, 1H, C*H*), 7.43 (d, *J* = 2.0 Hz, 1H, Ar-*H*), 7.27 (dd, *J* = 8.3 Hz, 2.0 Hz, 1H, Ar-*H*), 7.02 (d, *J* = 8.3 Hz, 1H, C*H*), 6.18 (t, *J* = 6.8 Hz, 1H, 1'-C*H*), 5.23 (d, *J* = 4.2 Hz, 1H, 3'-O*H*), 5.04 (t, *J* = 5.2 Hz, 1H, 5'-O*H*), 4.24 (dq, *J* = 6.2, 3.0 Hz, 1H, 3'-C*H*), 4.09 (q, *J* = 5.3 Hz, 2H, CH_2), 3.87 (s, 3H, OCH_3), 3.77 (q, *J* = 3.6 Hz, 1H, 4'-C*H*), 3.58 (d, *J* = 10.3 Hz, 2H, 5'-CH_2), 3.05 (q, J = 6.7 Hz, 2H, CH_2), 2.26 (t, *J* = 7.4 Hz, 2H, 2'-CH_2), 2.19 (tt, *J* = 5.5, 2.7 Hz, 2H, CH_2), 2.14 – 2.05 (m, 2H, CH_2), 1.96 (t, *J* = 7.1 Hz, 2H, CH_2), 1.56 (t, *J* = 7.3 Hz, 2H, CH_2).

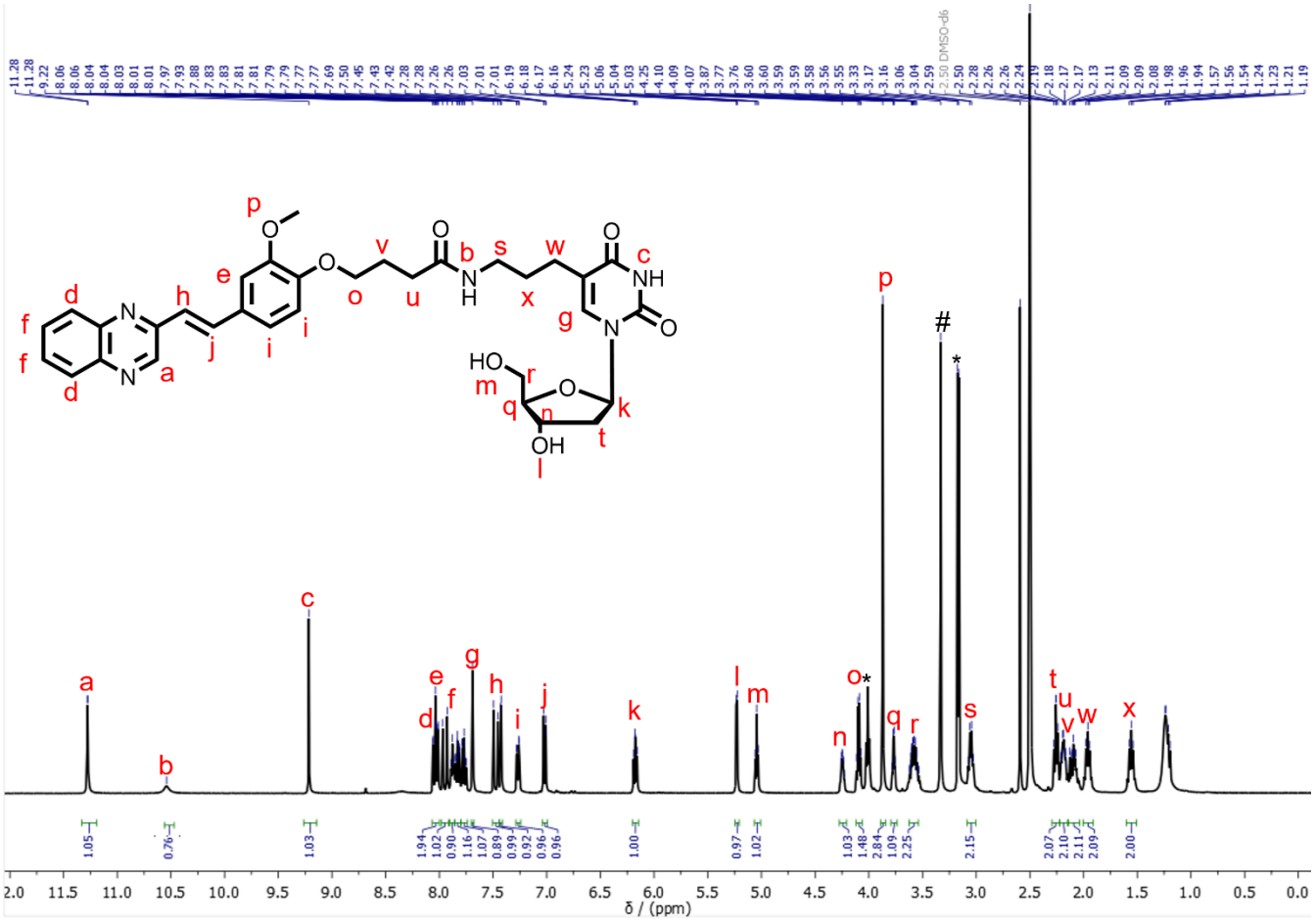

Figure S15: ^{1}H NMR spectrum of compound **4** (DMSO-d_6, 400 MHz, #: water, *: MeOH).

^{13}C-NMR (101 MHz, DMSO-d_6): δ (ppm) = 171.5 (*C*=O), 163.4 (*C*=O), 151.5 (*C*=O), 149.4 (*C*HO), 149.2 (*C*HO), 145.1 (*C*H-Ar), 141.8 (*C*H-Ar), 140.8 (*C*H-Ar), 136.6 (*C*H-Ar), 130.5 (*C*H), 129.2 (*C*H), 128.9 (*C*H-Ar), 128.8 (*C*H-Ar), 128.7 (*C*H-Ar), 123.2 (*C*H), 121.8 (*C*H-Ar), 113.0 (*C*H-Ar), 112.8 (*C*H-Ar), 110.0 (*C*H-Ar), 87.4 (1'-*C*H), 83.9 (4'-CH), 70.5 (3'-*C*H), 67.8 (CH_2), 61.4 (5'-CH_2), 55.6 (OCH_3), 39.1 (2'-CH_2), 37.8 (CH_2), 31.8 (CH_2), 28.0 (CH_2), 24.9 (CH_2), 23.9 (CH_2).

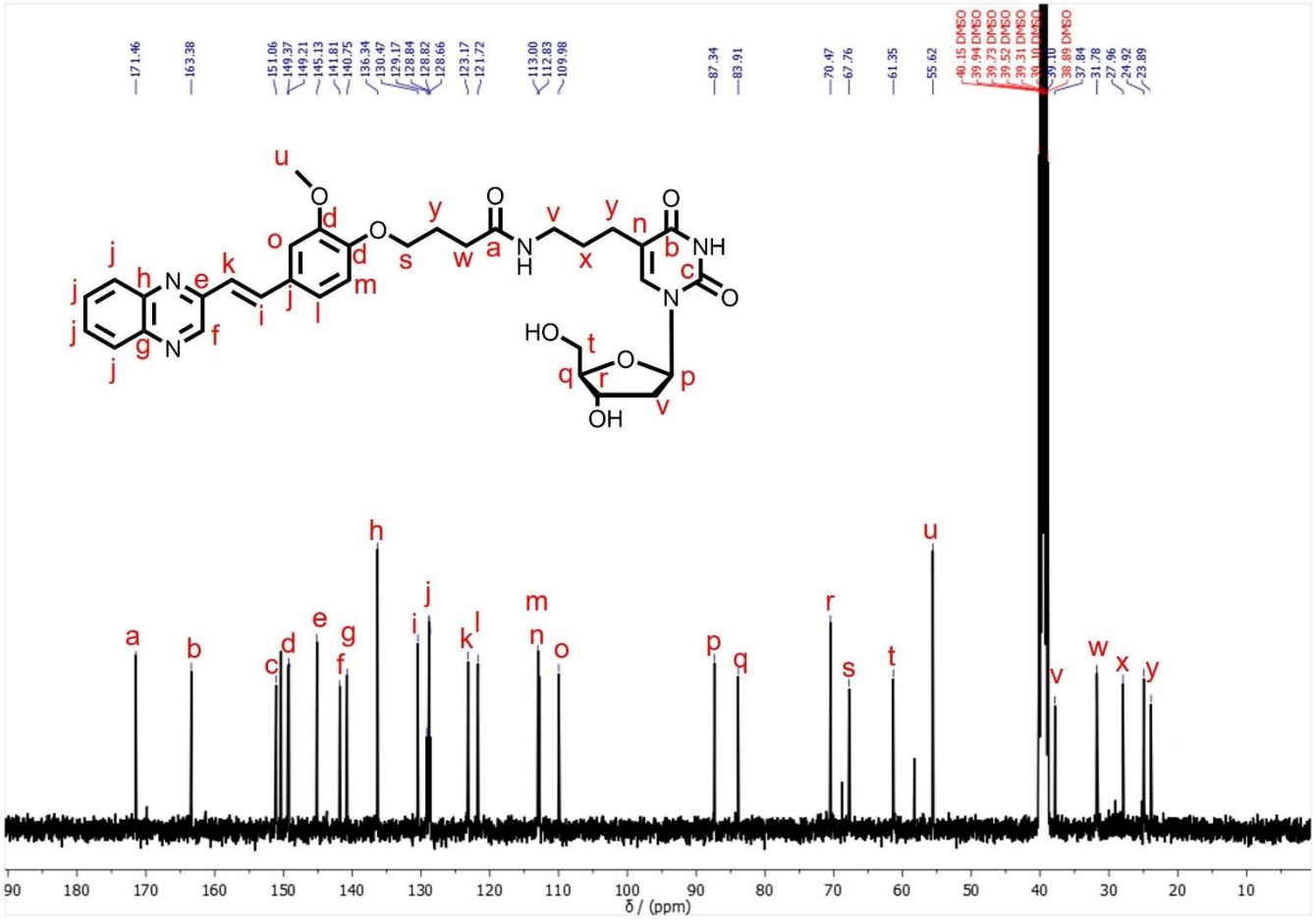

Figure S16: ^{13}C NMR spectrum of compound **4** (DMSO-d_6, 101 MHz).

ESI-HRMS: m/z calculated for $C_{33}H_{37}N_5O_8$ [M+Na]: 654.25422, meas.: 654.25286.

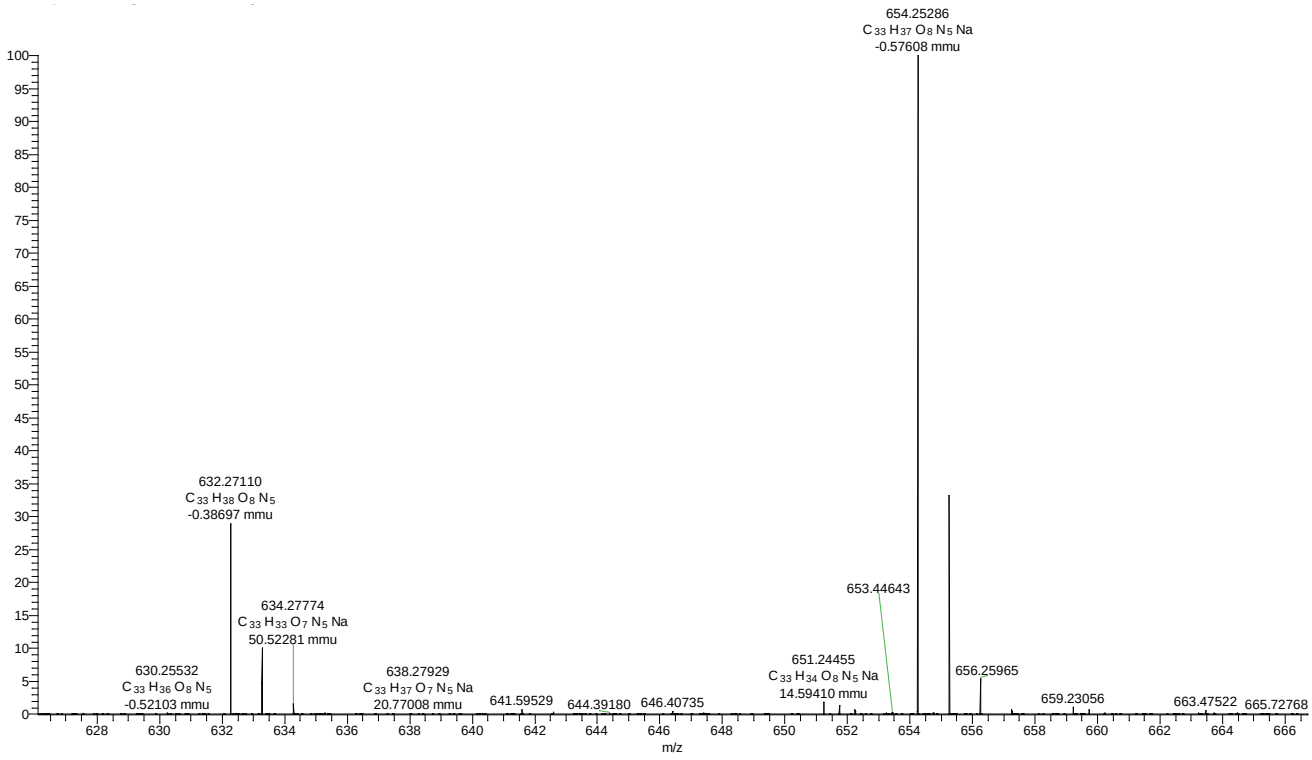

Figure S17: ESI-HRMS analysis of compound **4**: $M_{calc.}$ = 654.25422 g mol^{-1}, $M_{meas.}$ = 654.25286 g mol^{-1}.

3 Additional Spectra and Data

Compound **4** was further used to calculate the concentration of **DNA2.** Therefore, the extinction coefficient ε of **4** was determined, measuring absorbance spectra of different concentrations of **4** (**Figure S18**A)**.** The maxima were plotted vs. their correspondent concentration and linearly fitted (**Figure S18**B). The extinction coefficient ε was calculated using Beer-Lambert's law (A = εcd) and is ε_{260}= 11690 $M^{-1}cm^{-1}$.

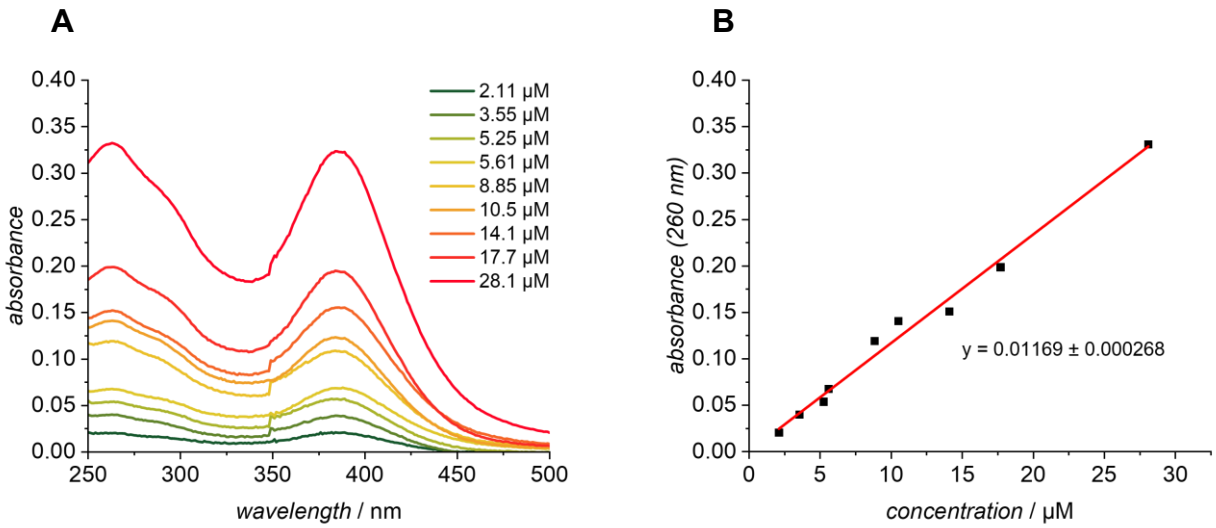

Figure S18: A: Absorbance spectra of different concentrations of **4**; **B:** Maxima plotted vs. their correspondent concentration and linearly fitted.

4 DNA Synthesis

4.1 Synthesis and Analysis of DNA1, DNA2 and $(DNA2)_2$

Table S1: Sequence, mass and retention time of synthesized oligonucleotides **DNA1**, **DNA2** and **$(DNA2)_2$**. HPLC: 0-50 % MeCN in NH_4OAc buffer at 40 °C in 30 min, followed by 10 min hold, flow: 1 ml min^{-1}.

Sample	Sequence	$M_{calc.}$ [g mol^{-1}]	$M_{meas.}$ [g mol^{-1}]	t_R [min]
DNA1	5'-GCA-GTC-TT**W**-TTC-ACT-GA-3'	5191.9	5193.7	-
DNA2	5'-GCA-GTC-TT**X**-TTC-ACT-GA-3'	5539.4	5540.0	13.2
$(DNA2)_2$	5'-GCA-GTC-TT**X'**-TTC-ACT-GA-3'	11078.8	-	12.8

Modified phosphoramidite **3** was incorporated into **DNA1** at a H-6 DNA/RNA Synthesizer from K&A Laborgeräte. CPG (1 µmol, 500 Å), phosphoramidites, reagents, solvents and columns which were used in DNA synthesis were purchased from ChemGenes, GlenResearch and Sigma Aldrich. Oligonucleotides were synthesized DMT-on. Conventional monomers were incorporated using standard conditions. Phosphoramidite **3** was used as 100 mM solution in MeCN with extended coupling time. The solution of the phosphoramidite is only stable for 24 h. After cleavage from the CPG (25% NH_4OH, 55 °C, 16 h) the oligonucleotides were purified by Glen-Pak™ DNA purification cartridge. Freeze drying gave **DNA1** as white powder.

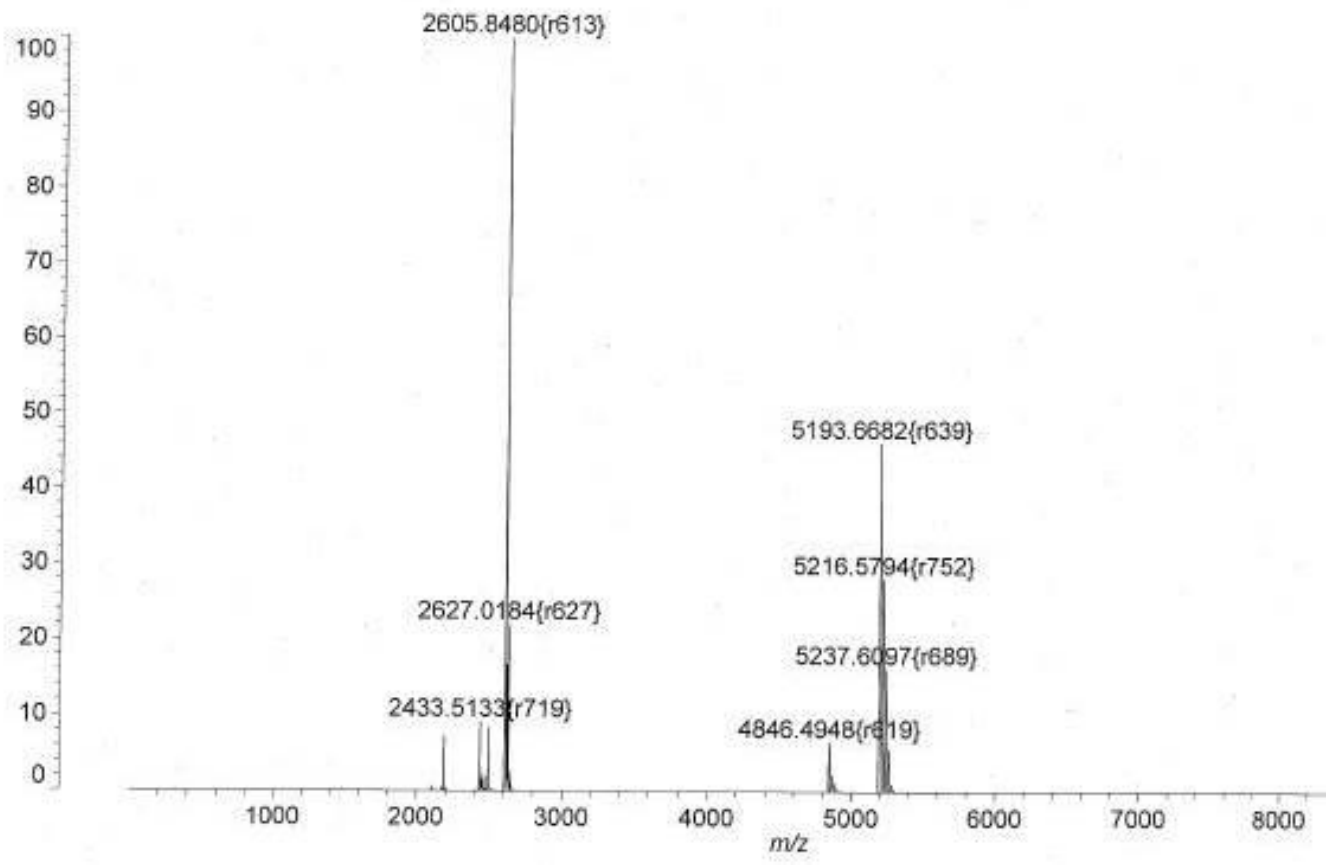

Figure S19: MALDI-TOF MS analysis of **DNA1**: $M_{calc.}$ = 5191.9 g mol^{-1}, $M_{meas.}$ = 5193.7 g mol^{-1}.

For the synthesis of **DNA2**, one strand **DNA1** (1 µmol, 1.00 equiv.) was dissolved in 100 µL ddH_2O and diluted in 100 µL anhydrous DMF and 10 µL DIPEA. To this solution was slowly added a solution of 1.38 mg SQ-NHS ester **1** (3 µmol, 3.00 equiv.) in 200 µL anhydrous DMF and the mixture was stirred at ambient temperature for 48 h. After removal of the solvent (refer to Chapter 1 "Freeze Drying"), the oligonucleotide was purified by HPLC. As column, a VDSphere OptiBio PUR 300 S18-SE-column (250×10 mm) was used. **DNA2** was detected by a DAD-3000 diode array detector at 260 nm and 290 nm (DNA absorbance) and 383 nm (SQ moiety absorbance). **DNA2** was obtained as a yellow powder. The modified oligonucleotide **DNA2** was quantified photometrically by absorption measurement at 260 nm at ND-100 spectrophotometer from Nanodrop, using calculated extinction coefficient ε_{260} of compound **4** (refer to chapter 3), characterized via UV/Vis spectroscopy and compared to nucleoside **4** (**Figure S20**). Nucleoside **4** shows a distinct band with two local maxima at around 270 nm and 383 nm that can be assigned to the SQ moiety. Apart from the maximum at 260 nm, **DNA2** also displays the SQ band at around 395 nm. The absorbance spectra of **DNA2** display a red-shift in the SQ absorbance band (from 383 nm to ca. 395 nm) in comparison to SQ-modified nucleoside **4**, which is likely associated with stacking interactions within the DNA molecule.

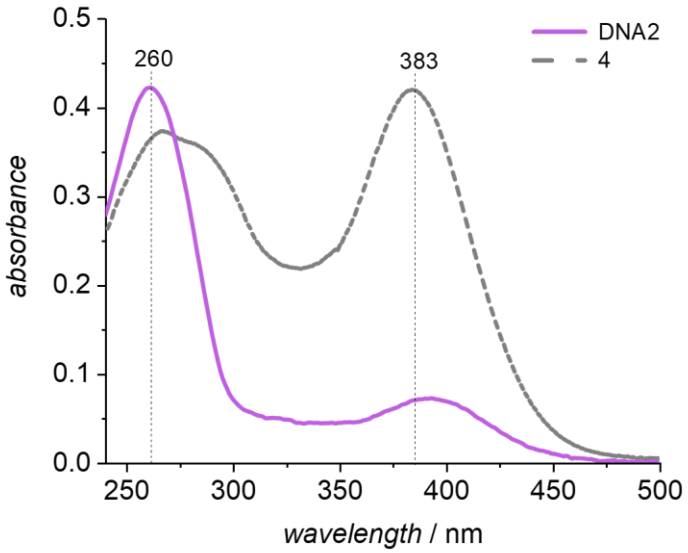

Figure S20: Normalised UV/Vis spectra of the oligonucleotide **DNA2** and nucleoside **4**. **DNA2**: 2.5 µM solution in 10 mM Na-P_i buffer with 250 mM NaCl at pH 7 at 20 °C, nucleoside **4**: 25 µM solution in H_2O at 20 °C.

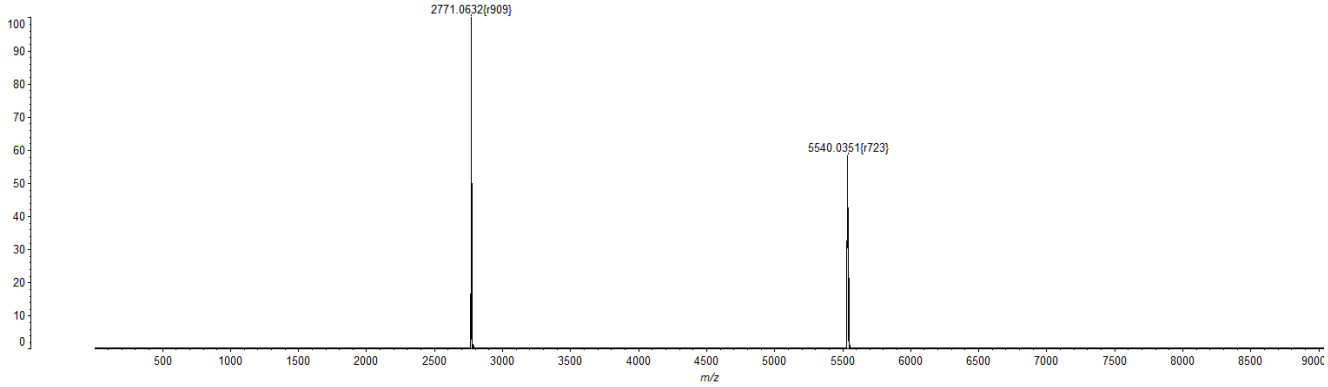

Figure S21: MALDI-TOF MS analysis of **DNA2**: $M_{calc.}$ = 5539.4 g mol^{-1}, $M_{meas.}$ = 5540.0 g mol^{-1}.

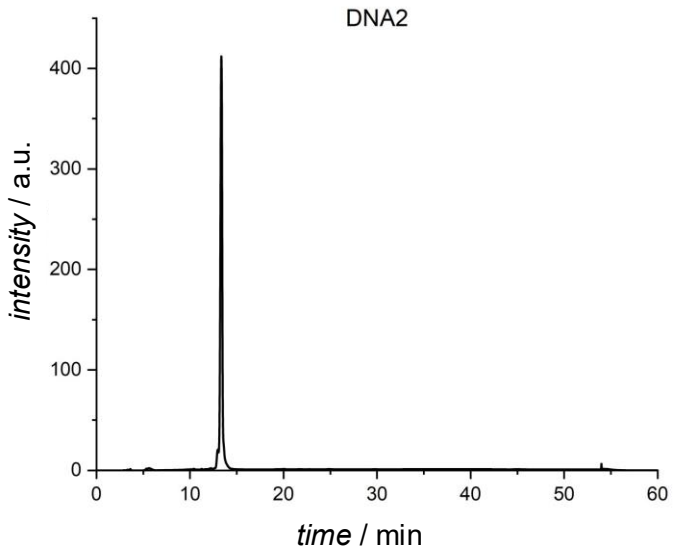

Figure S22: HPLC analysis of **DNA2**: t_R = 13.2 min.

Subsequently, irradiation experiments with synthesized **DNA2** were performed with a 450 nm LED to obtain homo-dimerized **$(DNA2)_2$**. Irradiation experiments were performed using 50 µM **DNA2** in H_2O, 10 mM Na-P_i buffer and 250 mM NaCl in a total volume of 600 µL in a crimp vial. LEDs (Duris E2835, GD JTLPS1.14) were purchased at Osram and the mixture was irradiated from the bottom of the vial under continuous stirring and constant temperature of 20 °C. Cooling of the reaction was performed using a Lauda Alpha R 8 thermostat.

4.2 Analytical HPLC Analysis of $(DNA2)_2$

Analytical HPLC analysis of the irradiation reaction of **DNA2** to **$(DNA2)_2$** was performed at $\lambda_{detection}$=260 nm (DNA absorbance maximum), further confirming the formation of the homo-dimerized **$(DNA2)_2$**. Pre-irradiation, the chromatogram of **DNA2** shows one significant peak at t_R = 13.1 min (**Figure S23**, dark green line). During irradiation, the peak decreases while a new peak at t_R = 12.6 min (**Figure S23**, red line) is formed.

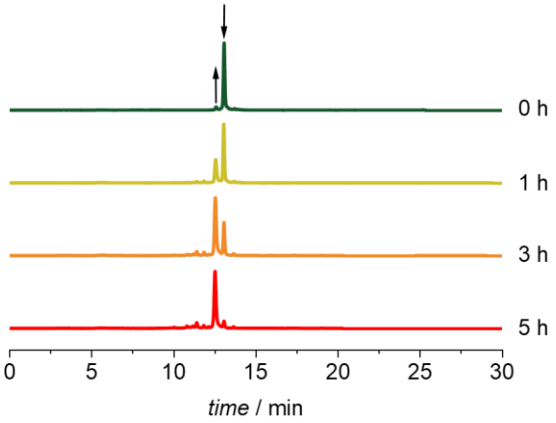

Figure S23: RP-HPLC analyses ($\lambda_{detection}$=260nm) of 50 µM **DNA2** over 5 h of irradiation at 20 °C with a 450 nm LED in H_2O, 10 mM Na-P_i buffer and 250 µM NaCl.

However, mass spectrometric analyses (MALDI-TOF, ESI-HRMS and ESI-LC-MS) do not confirm the formation of **$(DNA2)_2$**. The dimerized oligonucleotide **$(DNA2)_2$** might be challenging to ionize during mass spectroscopic analyses. Thus, agarose gel electrophoresis was carried out (Manuscript, Figure 2B). After successful homo-dimerization of **DNA2**, **$(DNA2)_2$** is expected to feature double the mass of **DNA2** and thus a slower electrophoretic mobility since the strands are connected through successful [2+2] cycloaddition between two SQ moieties (Manuscript, Scheme 1d).

4.3 Synthesis and analysis of DNA3

Table S2: Sequence, mass and retention time of synthesized oligonucleotides **DNA1**, **DNA2**, **(DNA2)$_2$** and **DNA3**. HPLC: 0-50 % MeCN in NH_4OAc buffer at 40 °C in 30 min, followed by 10 min hold, flow: 1 ml min^{-1}.

Probe	Sequence	$M_{calc.}$ [g mol^{-1}]	$M_{meas.}$ [g mol^{-1}]	t_R [min]
DNA1	5'-GCA-GTC-TT**W**-TTC-ACT-GA-3'	5191.9	5193.7	-
DNA2	5'-GCA-GTC-TT**X**-TTC-ACT-GA-3'	5539.4	5540.0	13.2
(DNA2)$_2$	5'-GCA-GTC-TT**X'**-TTC-ACT-GA-3'	11078.8	-	12.8
DNA3	5'-GCA-GTC-TT**Y**-TTC-ACT-GA-3'	6456.5	-	18.5, 19.2

4.3.1 DNA3 (1:1 equivalents)

After successful homo-dimerization of **DNA2** to **(DNA2)$_2$**, hetero-dimerization of SQ-modified **DNA2** with synthesized SQ-modified Atto655 dye **2** to **DNA3** through irradiation for 1 to 5 h with a 450 nm LED was investigated. Initial experiments were performed using 50 µM **DNA2** and 50 µM SQ-modified Atto 655 dye **2** (stock solution in DMF due to poor solubility in H_2O) in aqueous solution, containing 5% DMF, 10 mM Na-P_i buffer and 250 mM NaCl in a total volume of 600 µL in a crimp vial. LEDs (Duris E2835, GD JTLPS1.14) were purchased at Osram and the mixture was irradiated from the bottom of the vial under continuous stirring and constant temperature of 20 °C. Cooling of the reaction was performed using a Lauda Alpha R8 thermostat. Absorbance spectra (**Figure S24**) and HPLC chromatograms (**Figure S25**) initially displayed inconclusive results since **DNA2** and **DNA3** showed predominantly similar spectra, making differentiation of the oligonucleotides challenging.

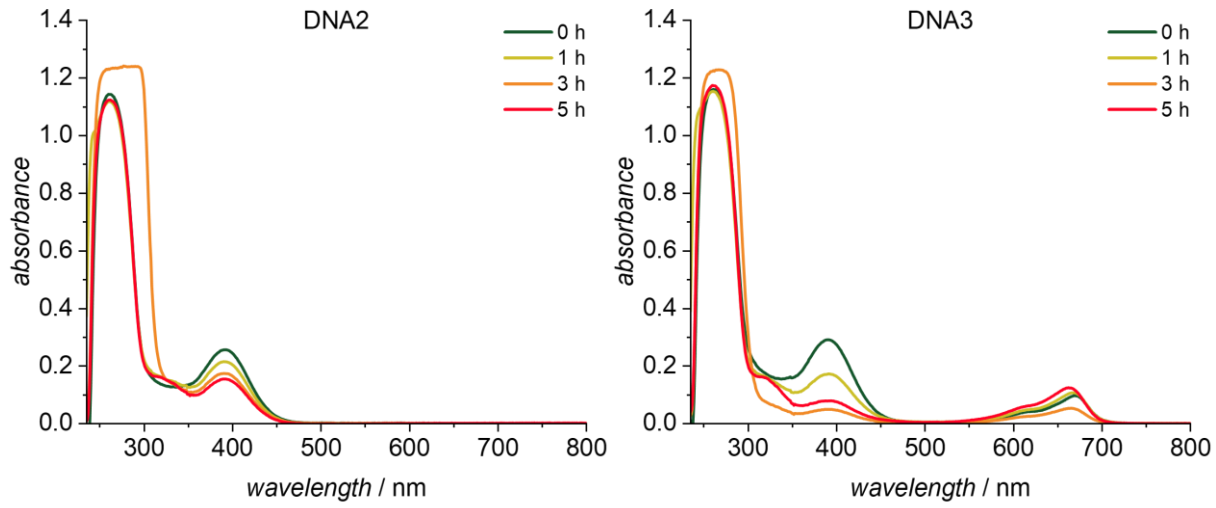

Figure S24: UV/Vis spectroscopic analysis of **DNA2** and **DNA3** (1:1 equiv.) after irradiation with a 450 nm LED in aqueous media containing 5% DMF, 10 mM Na-P_i buffer and 250 mM NaCl in a total volume of 600 µL in a crimp vial for 5 h at 20 °C. **DNA2** and **DNA3** both show – pre-irradiation (dark green line) – two distinctive absorbance maxima at λ_{max1}=260 nm, associated with the DNA absorbance and λ_{max2}=383 nm, associated with the SQ-moiety. Furthermore, **DNA3** shows a third maximum at λ_{max2}=655 nm, that can be assigned to the SQ-modified Atto655 dye. During irradiation, one new maximum is emerging at λ=325 nm whereas the assigned SQ maximum is decreasing (red line). Nevertheless, **DNA2** and **DNA3** show similar change in absorbance after 5 h of irradiation with a 450 nm LED, making clear conclusion about formation of **DNA3** difficult.

Analytical HPLC analysis was performed at $\lambda_{detection}$=260 nm.

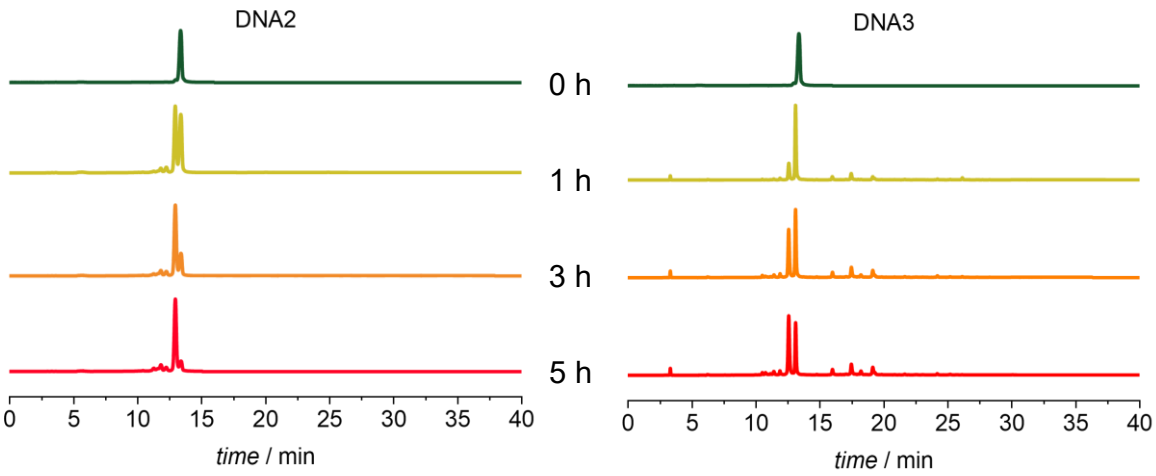

Figure S25: HPLC analysis of **DNA2** and **DNA3** (1:1 equiv.) after irradiation for 5 h in total with a 450 nm LED in aqueous media containing 5% DMF, 10 mM Na-P_i buffer and 250 mM NaCl in a total volume of 600 µL in a crimp vial at 20 °C. Pre-irradiation, the chromatograms of both **DNA2** and **DNA3** show one significant peak at t_R = 13.1 min (dark green line). During irradiation, the peak decreases while a new peak at t_R = 12.6 min (red line) is formed. As the formation of the new peak at t_R = 12.8 min is not as significant in **DNA3** as it is in **DNA2**, possible reaction with SQ-modified Atto dye **2** could be suggested. Nevertheless, clear confirmation of formation of **DNA3** is not possible since the results are quite similar.

Thus, agarose gel electrophoresis was selected for the investigation of the reaction of **DNA2** to **DNA3**. **DNA3** displays a mass between **DNA2** and **$(DNA2)_2$** (see **Table S2**) and is therefore expected to lead a band between these two fragments, indicating successful reaction with the SQ-modified Atto655 **2**. The agarose gel (**Figure S26**) shows four lanes in total. Lane 1 displays the commercially available DNA marker and lane 2 represents non-irradiated **DNA2.** The last two lanes are filled with **$(DNA2)_2$** (lane 3) and **DNA3** (lane 4) after 5 h of irradiation with a 450 nm LED.

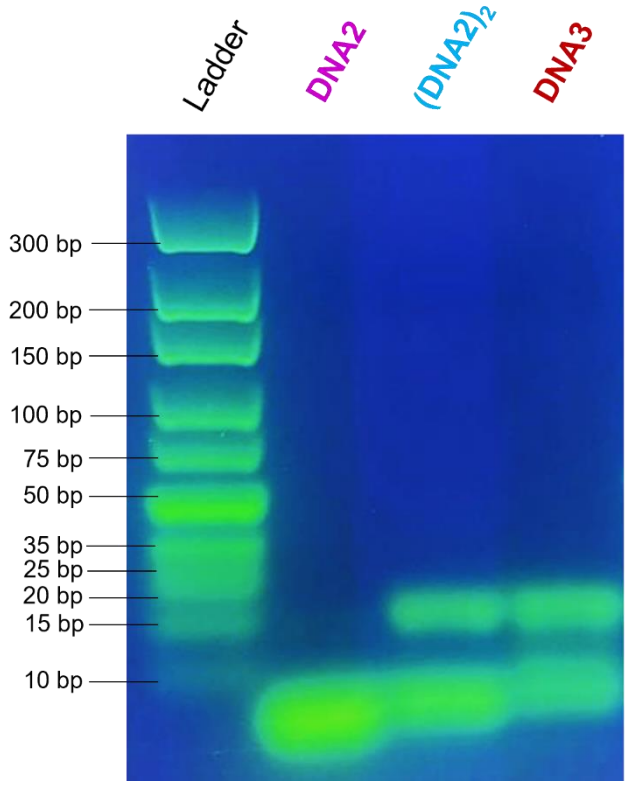

Figure S26: Agarose gel electrophoretic analysis of **DNA3** (1:1 equiv.) after irradiation at λ_{max}=450 nm in aqueous media containing 5% DMF, 10 mM Na-P_i buffer and 250 mM NaCl in a total volume of 600 µL in a crimp vial for 5 h at 20 °C. Staining was performed using SybrGreen, followed by visualization under UV light (λ_{exc}=312 nm). Lane 1: commercial DNA marker, lane 2: **DNA2** (pre-irradiation), lane 3: **$(DNA2)_2$**, lane 4: **DNA3**.

Lane 2 (**DNA2**) displays one gel band with the smallest size of all three lanes. **(DNA2)$_2$** in lane 3 shows two gel bands, one in the same position as lane 2 and one located between 15 and 20 bp in comparison to the marker in lane 1. The smaller sized fragment can be assigned to starting material **DNA2** whereas the larger sized fragment describes the dimerization product of **DNA2** to **(DNA2)$_2$**. **DNA3** was expected to feature a band between **DNA2** and **(DNA2)$_2$**. However, lane 4 displays the same two fragments as lane 3, indicating no reaction between **DNA2** and the SQ-modified Atto dye **2**.

In addition, denaturing polyacrylamide gel electrophoresis (PAGE) was performed as a more sensitive method than agarose gel electrophoresis. **DNA3** is expected to lead to a band between **DNA2** and **(DNA2)$_2$** as explained in **Figure S26**. The PAGE (**Figure S27**) shows three lanes in total. Lane 1 displays non-irradiated **DNA2,** whereas lanes 2 and 3 represent **(DNA2)$_2$** and **DNA3** after 5 h of irradiation with a 450 nm LED. As stated by the supplier of the ladder, double stranded ladders are not recommended for denaturing electrophoresis as they may form an atypical pattern.

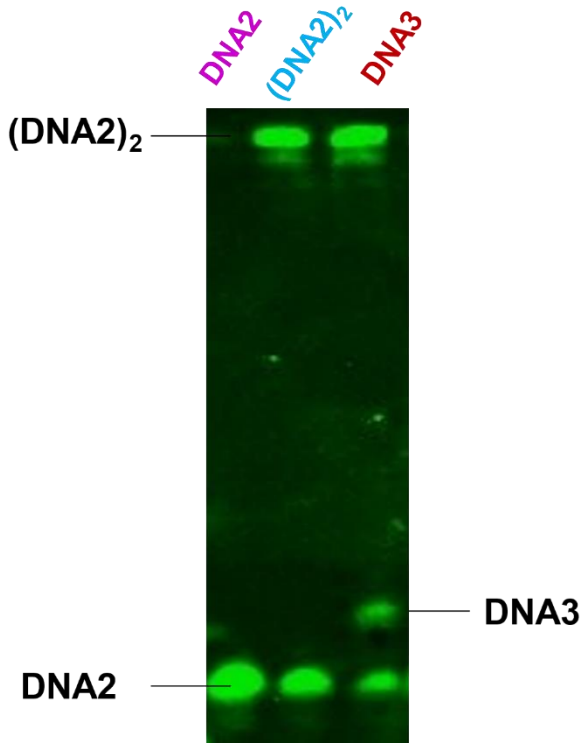

Figure S27: Denaturing PAGE analysis of **DNA3** (1:1 equiv.) after irradiation at λ_{max}=450 nm in aqueous media containing 5% DMF, 10 mM Na-P$_i$ buffer and 250 mM NaCl in a total volume of 600 µL in a crimp vial for 5 h at 20 °C. Staining was performed using SybrGreen, followed by visualization under UV light (λ_{exc}=312 nm). Lane 1: non-irradiated **DNA2**, lane 2: homo-dimerized **(DNA2)$_2$**, lane 3: **DNA3**.

Lane 1 (**DNA2** pre-irradiation) displays one gel band with the smallest size of all three lanes. **(DNA2)$_2$** in lane 2 shows two gel bands, one in the same position as lane 2 and one located at the upper end of the gel. The smaller sized fragment can be assigned to starting material **DNA2**, whereas the larger sized fragment is associated with the dimerization product of **DNA2** to **(DNA2)$_2$**. **DNA3** is expected to feature a band between **DNA2** and **(DNA2)$_2$**. Lane 3 displays the same two fragments as lane 2, but also a faint new band between **DNA2** and **(DNA2)$_2$**, indicating reaction between **DNA2** and the SQ-modified Atto dye **2**. Nevertheless, conversion of **DNA2** to homo-dimerized **(DNA2)$_2$** is favoured to conversion of **DNA2** to **DNA3**.

In addition to the favoured reaction of **DNA2** to **$(DNA2)_2$** using a 1:1 ratio, there is also evidence of homo-dimerization between two SQ-modified Atto655 dyes, demonstrated by irradiation of 50 µM SQ-modified Atto655 dye **2** (stock solution in DMF due to poor solubility in H_2O) in aqueous solution, containing 5% DMF, 10 mM Na-P_i buffer and 250 mM NaCl in a total volume of 600 µL in a crimp vial for 5 h at 20 °C with a 450 nm LED. LEDs (Duris E2835, GD JTLPS1.14) were purchased at Osram and the mixture was irradiated from the bottom of the vial under continuous stirring and constant temperature of 20 °C. Cooling of the reaction was performe d using a Lauda Alpha R8 thermostat. Absorbance spectra (**Figure S28**) and ESI-HRMS (**Figure S29**) confirmed conversion of monomer Atto655 dye **2** to homo-dimerized Atto655 dye **$(2)_2$**.

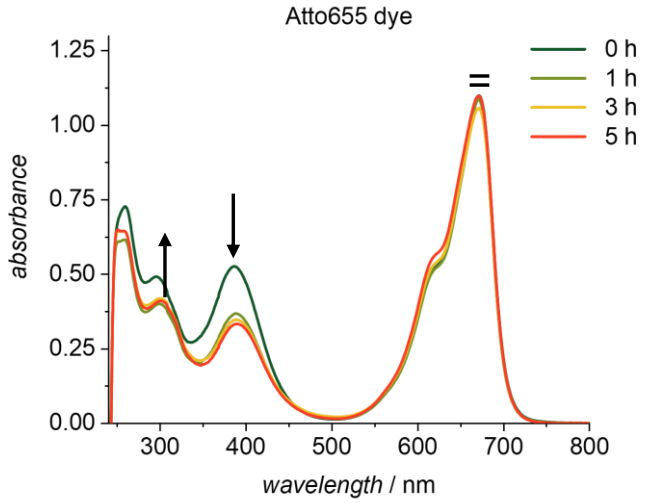

Figure S28: UV/Vis spectroscopic analysis of 50 µM SQ-modified Atto655 dye **2** after irradiation with a 450 nm LED in aqueous media containing 5% DMF, 10 mM Na-P_i buffer and 250 mM NaCl in a total volume of 600 µL in a crimp vial for 5 h at 20 °C. The Atto655 dye shows – pre-irradiation (dark green line) – four distinctive absorbance maxima at λ_{max1}=260 nm, λ_{max2}=298 nm and λ_{max3}=384 nm associated with the SQ-moiety as well as λ_{max4}=655 nm, which displays the excitation maximum of the Atto655 dye. During irradiation, one new maximum is emerging at λ=325 nm whereas the assigned SQ maximum at λ=384 nm is decreasing (red line). The assigned Atto655 maximum at λ_{max4}=655 nm remains unchanged, confirming the stability of the dye after 5 h of irradiation with 450 nm LED.

After successful reaction of SQ-modified Atto655 dye **2** with itself to homo-dimerized Atto655 dye **$(2)_2$** through visible light-induced [2+2] cycloaddition, the resulting product features double the molecular weight, confirmed via ESI-HRMS (**Figure S28**).

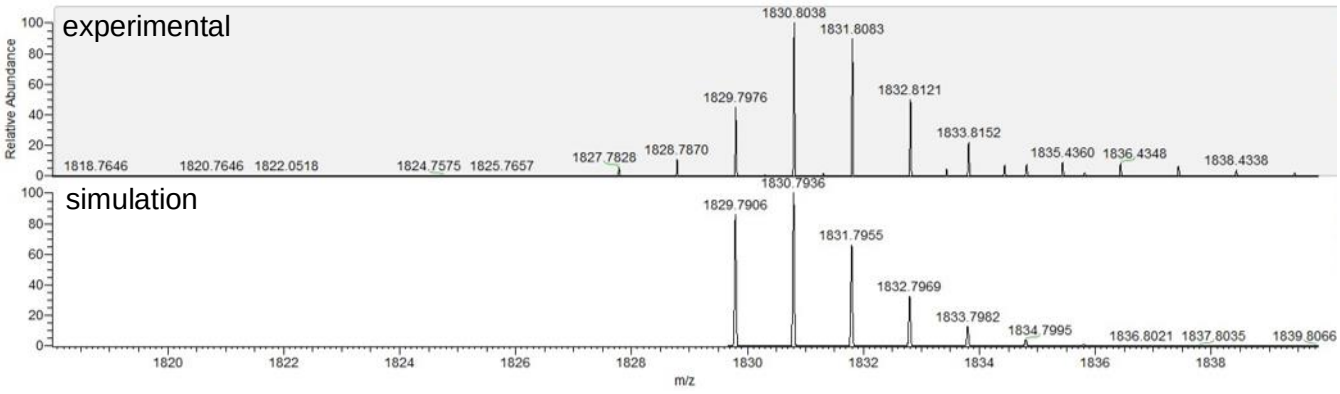

Figure S29: ESI-HRMS analysis of homo-dimerized Atto655 dye **$(2)_2$**: $M_{calc.}$ = 1829.7906 g mol^{-1} [$C_{100}H_{113}N_{14}O_{16}S_2^-$], $M_{meas.}$ = 1829.7976 g mol^{-1} [$C_{100}H_{113}N_{14}O_{16}S_2^-$].

Although occurring as a competing reaction, the homo-dimerization between two fluorophore dyes was neither detectable though gel electrophoresis due to too low molecular weight nor distinguishable from hetero-dimerization of **DNA2** to **DNA3** in UV/Vis spectra (compare **Figure S24** right, **Figure S30** right). As this reaction is not interfering with the DNA strand itself, it is of minor concern.

4.3.2 DNA3 (1:5 equivalents)

To shift the reaction towards hetero-dimerization (formation of **DNA3**) instead of homo-dimerization (formation of **$(DNA2)_2$**), we repeated the previous experiment, irradiating 50 µM **DNA2** and 250 µM SQ-modified Atto655 dye **2** (stock solution in DMF due to poor solubility in H_2O) in aqueous solution, containing 5% DMF, 10 mM Na-P_i buffer and 250 mM NaCl in a total volume of 600 µL in a crimp vial with a 450 nm LED for 5 h at 20 °C.
Absorbance spectra of **DNA3** initially showed inconclusive results (**Figure S30**), displaying similar change in absorbance of the SQ moiety as absorbance spectra of **$(DNA2)_2$.**

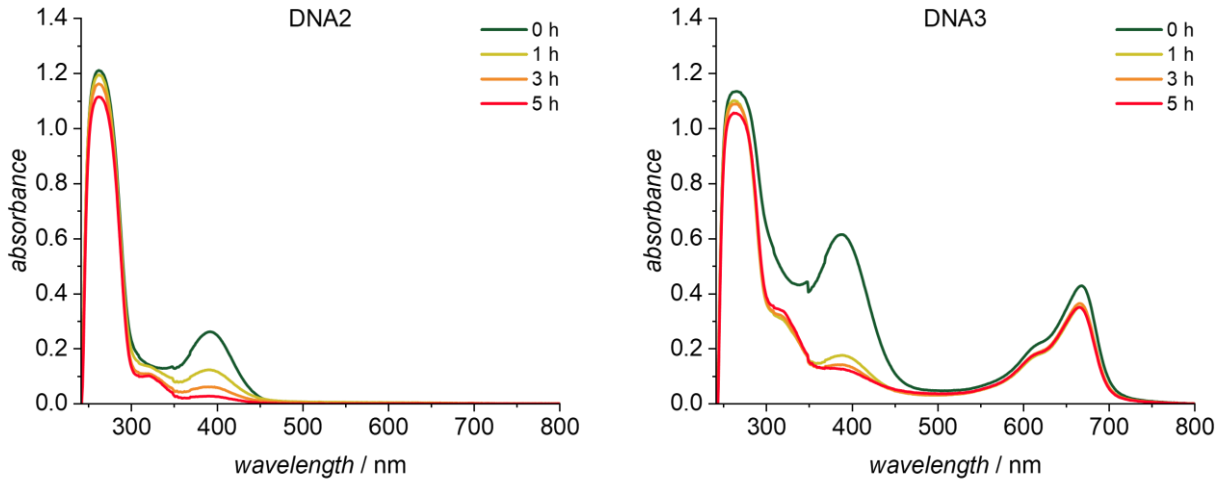

Figure S30: UV/Vis spectroscopic analysis of **DNA2** and **DNA3** (1:5 equiv.) after irradiation with a 450 nm LED in aqueous media containing 5% DMF, 10 mM Na-P_i buffer and 250 mM NaCl in a total volume of 600 µL in a crimp vial for 5h at 20 °C. **DNA2** and **DNA3** both show – pre-irradiation (dark green line) – two distinctive absorbance maxima at λ_{max1}=260 nm, associated with the DNA absorbance and λ_{max2}=383 nm, associated with the SQ-moiety. Furthermore, **DNA3** shows a third maximum at λ_{max3}=655 nm, that can be assigned to the SQ-modified Atto655 dye. During irradiation, one new maximum is emerging at λ=325 nm whereas the assigned SQ maximum is decreasing (red line). Nevertheless, **DNA2** and **DNA3** show similar change in absorbance after 5 h of irradiation with 450 nm LED, making clear conclusion about formation of **DNA3** difficult.

This time, the detection wavelengths for HPLC analysis of **DNA3** were set to $\lambda_{detection1}$=260 nm (DNA absorbance maximum, **Figure S31** left) and $\lambda_{detection2}$=650 nm (Atto655 absorbance maximum, **Figure S31** right). At $\lambda_{detection}$=260 nm HPLC chromatograms display peaks of **DNA2** at t_R = 13.2 min and **(DNA2)$_2$** at t_R = 12.8 min. Four new peaks are forming and increasing over the course of irradiation at t_R = 15.9, 17.4, 18.5 and 19.2 min.

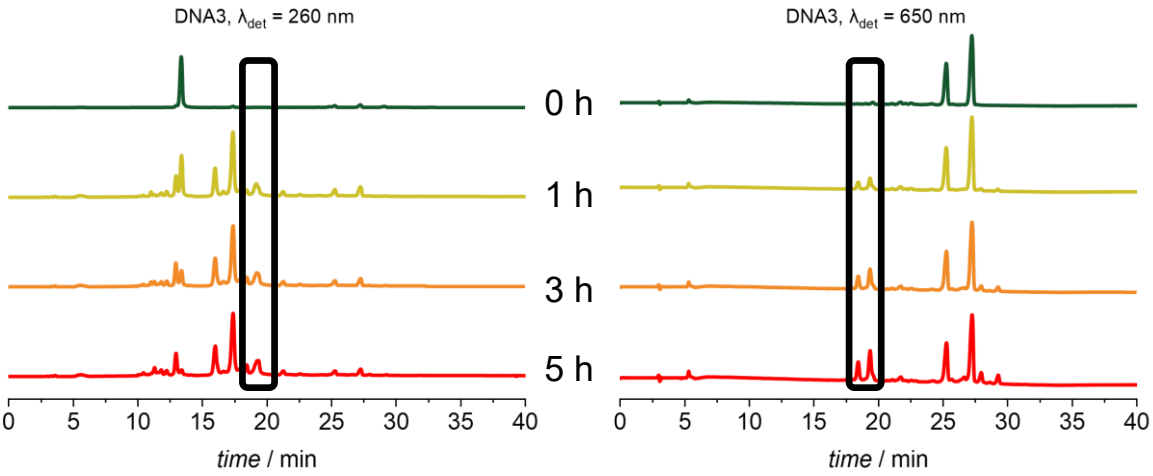

Figure S31: HPLC analysis of **DNA3** (1:5 equiv.) after irradiation with a 450 nm LED in aqueous media containing 5% DMF, 10 mM Na-P_i buffer and 250 mM NaCl in a total volume of 600 µL in a crimp vial for 5h at 20 °C, detection wavelength = 260 nm (left). The signals at t_R ~ 13 min represent **DNA2/(DNA2)$_2$**. Four new peaks are forming and increasing over the course of irradiation at t_R = 15.9, 17.4, 18.5 and 19.2 min. The last two peaks (t_R = 25 and 27 min) at $\lambda_{detection}$=650 nm (right) are assigned to the SQ-modified Atto655 dye. As two new peaks develop and increase at t_R = 18.5 and 19.2 min (black circle), both showing absorbance at λ_1=260 nm and λ_2=650 nm, they can be assigned to formation of **DNA3**.

At $\lambda_{detection}$ = 650 nm, the last two peaks at t_R = 25 min and 27 min are assigned to the SQ-modified Atto655 dye. Two new peaks develop and increase at t_R= 18.5 and 19.2 min over 5 h of irradiation time. These peaks show both absorbance at λ=260 nm and λ=655 nm and can therefore be assigned to formation of **DNA3.**

However, the HPLC results of **DNA3** are not as convincing as HPLC analyses of homo-dimerization to **(DNA2)$_2$**. Thus, agarose gel electrophoresis (Manuscript, Scheme 2b) was selected as complementary method to confirm the ligation of **DNA2** to **DNA3.**

The yield of **DNA3** was determined via Image Analyzer v.450 of Raytest Company through comparison of gel band intensities of denaturing gel electrophoresis (PAGE), providing the percentage of integrated peak areas. For completeness, all collected samples were assembled in one gel (**Figure S32** left). Lane 1 shows **DNA2** after 1 h of irradiation time (homo-dimerization to **$(DNA2)_2$**), whereas lanes 2 to 4 show **DNA3** after 1 h, 3 h and 5 h irradiation time (hetero-dimerization).

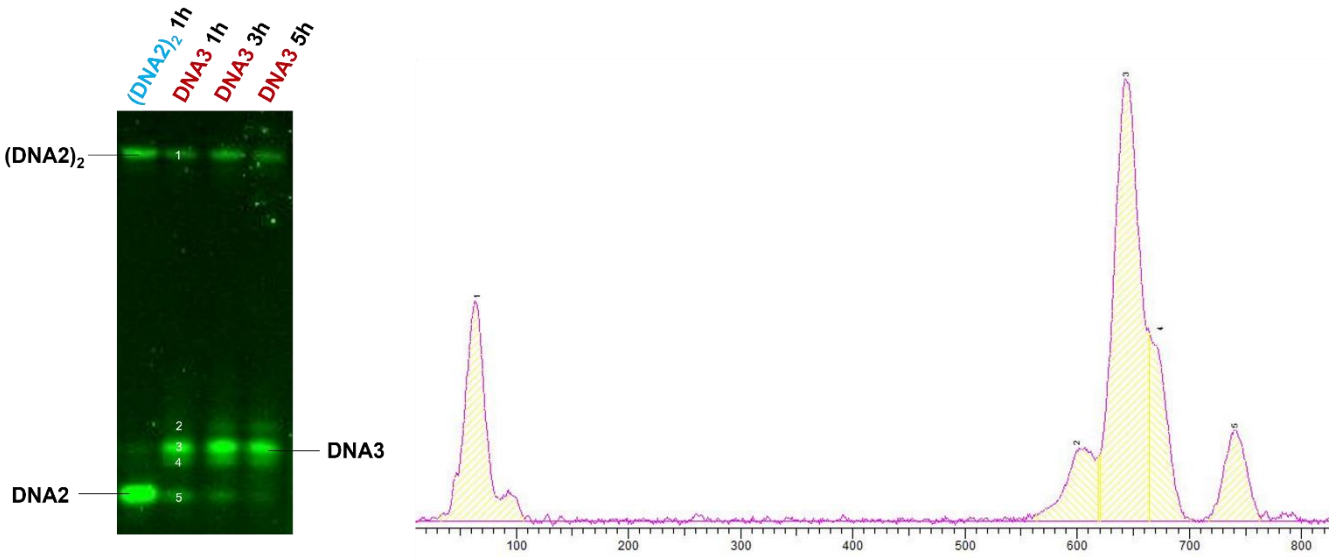

Figure S32: PAGE analysis (left) and yield determination (right) of **DNA3**.

By comparison of 1 h irradiation time of **DNA3** (**Figure S32** left, lane 2) to 5 h irradiation time (**Figure S32** left, lane 4), it is clearly visible that 1 h of irradiation time is sufficient to build **DNA3** as the band intensities are similar. The software for the yield determination recognized five bands in total (**Figure S32** right). After 1 h of irradiation, the following yields were determined (**Table S3**).

Table S3: Determined yields after irradiation of **DNA2** and five-fold excess of SQ-modified Atto655 dye 2 for 1 h with 450 nm LED.

Product	Yield [%]
DNA2	24
DNA3	58
$(DNA2)_2$	18

In conclusion, after 1 h of irradiation of **DNA2** with five-fold excess of SQ-modified Atto655 dye **2**, 58% of the starting material (**DNA2**) are converted to **DNA3** whereas 18% undergo reaction to homo-dimerized **$(DNA2)_2$.**

4.4 Synthesis and Analysis of DNA4

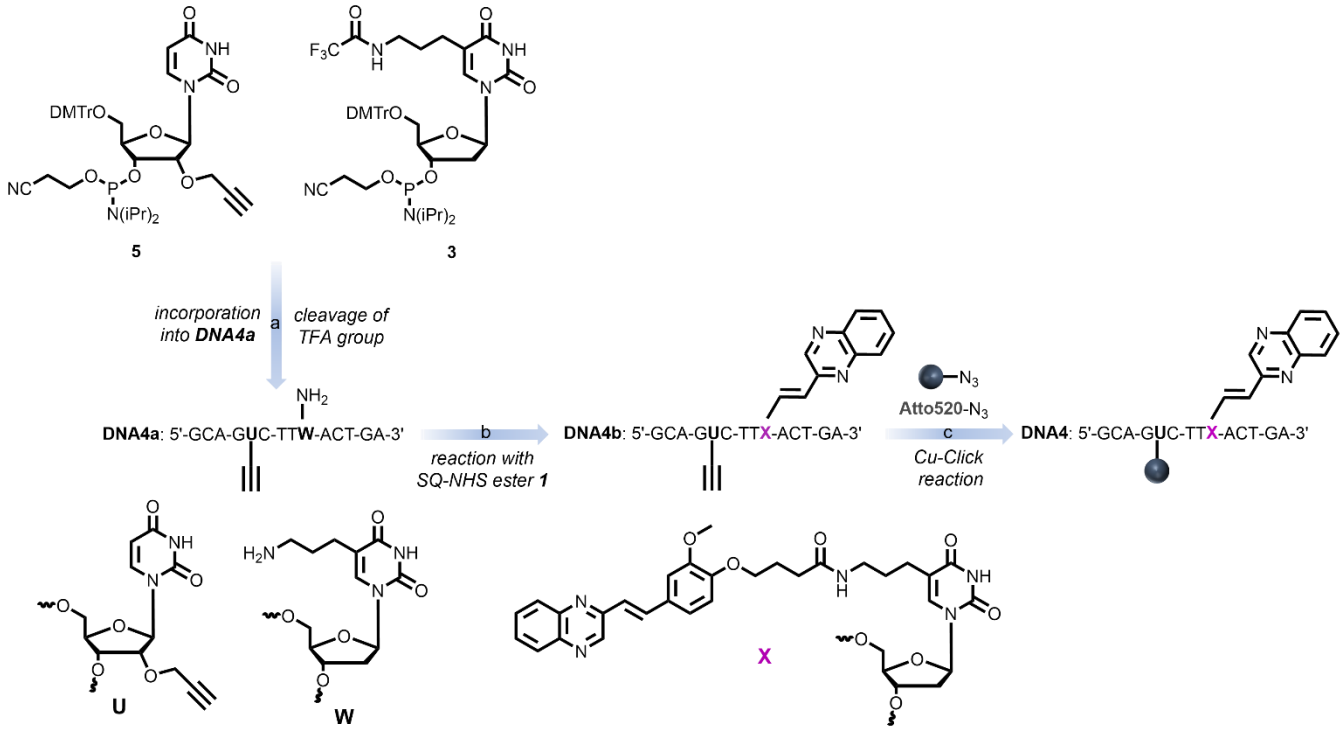

Scheme S3: Synthesis of **DNA4**: a.) Incorporation of **5** and **3** into **DNA4a** via DNA synthesizer, followed by cleavage of TFA group with 25% NH_4OH, 55 °C, 16 h; b.) Synthesis of **DNA4b**: **1**, DIPEA, DMF, r.t., 48 h; c.) Synthesis of **DNA4** through Cu(I)-Click reaction with commercially available Atto520-N_3.

Table S4: Sequence, mass and retention time of synthesized oligonucleotides **DNA4a**, **DNA4b** and **DNA4**. HPLC: 0-20 % MeCN in NH_4OAc buffer at 40 °C in 30 min, followed by 10 min hold, flow: 2.5 ml min^{-1}.

Probe	Sequence	M_{calc} [g mol^{-1}]	$M_{meas.}$ [g mol^{-1}]	t_R [min]
DNA4a	5'-GCA-G**U**C-TT**W**-ACT-GA-3'	4334.2	4329.9	-
DNA4b	5'-GCA-G**U**C-TT**X**-ACT-GA-3'	4681.5	4678.9	29.0
DNA4	5'-GCA-G**U**C-TT**X**-ACT-GA-3'	5257.7	5256.1	40.8

4.4.1 Synthesis of DNA4a

DNA4 was synthesized via a three-step procedure, starting with the incorporation of modified phosphoramidite building block **3** and simultaneous incorporation with commercially available phosphoramidite **5** into **DNA4a** (**Scheme S3**a). Phosphoramidites **3** and **5** were each used as 100 mM solution in MeCN (the solution of each phosphoramidite is only stable for 24 h) with extended coupling time. After cleavage from the CPG (25% NH_4OH, 55 °C, 16 h) the oligonucleotides were purified by Glen-Pak™ DNA purification cartridge. After freeze drying, **DNA4a** was obtained as white powder.

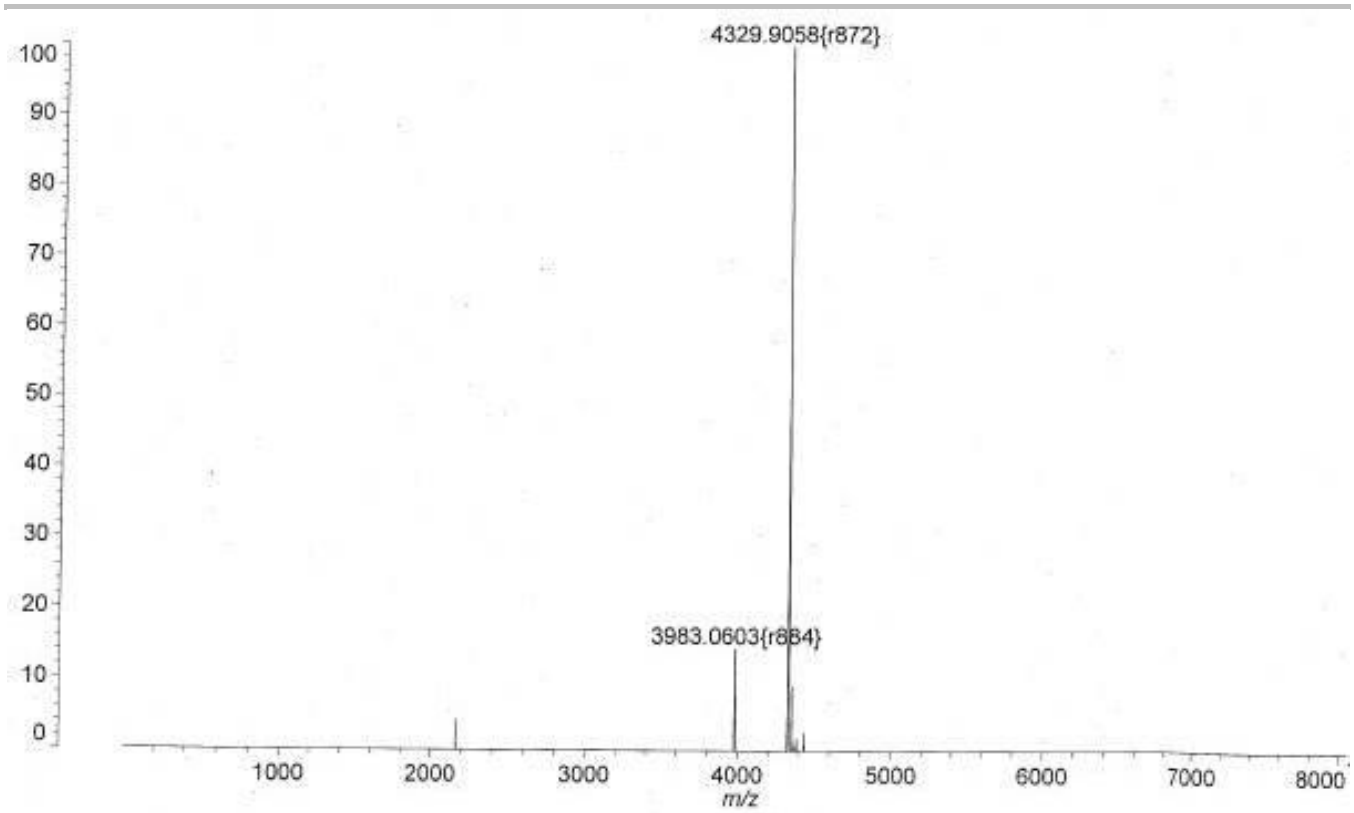

Figure S33: MALDI-TOF MS analysis of **DNA4a**: $M_{calc.}$ = 4334.2 g mol^{-1}, $M_{meas.}$ = 4329.9 g mol^{-1}.

4.4.2 Synthesis of DNA4b

For synthesis of **DNA4b** (**Scheme S3**b), five strands **DNA4a** (5 µmol, 1.00 equiv.) were dissolved in 200 µL ddH_2O and diluted in 200 µL anhydrous DMF and 20 µL DIPEA. To this solution was slowly added a solution of 6.92 mg SQ-NHS ester **1** (15 µmol, 3.00 equiv.) in 500 µL anhydrous DMF and the mixture was stirred at ambient temperature for 48 h. After removal of the solvent (refer to Chapter 1 "Freeze Drying"), the oligonucleotide was purified by HPLC (**Figure S34**). As column, a VDSphere OptiBio PUR 300 S18-SE-column (250×10 mm) was used. **DNA2** was detected by a DAD-3000 diode array detector at 260 nm and 290 nm (DNA absorbance) and 383 nm (SQ moiety absorbance). **DNA4b** was obtained as a yellow powder after freeze drying.

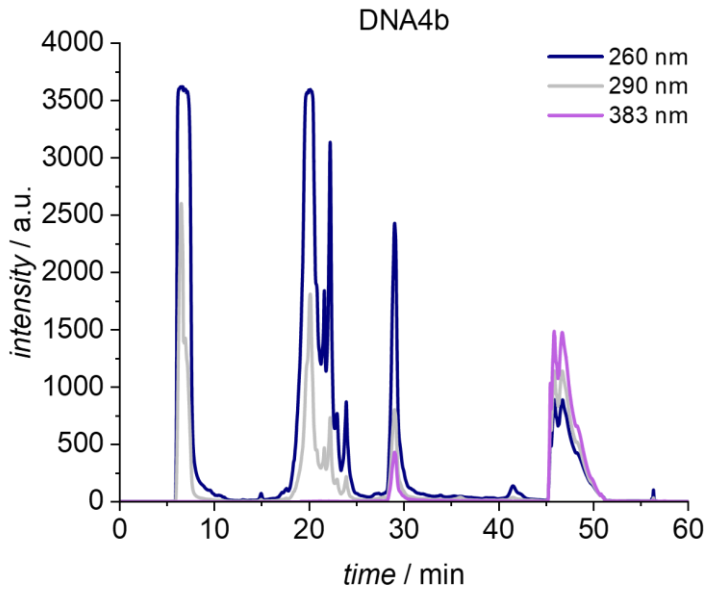

Figure S34: Semi-preparative HPLC analysis of **DNA4b:** t_R = 29.0 min.

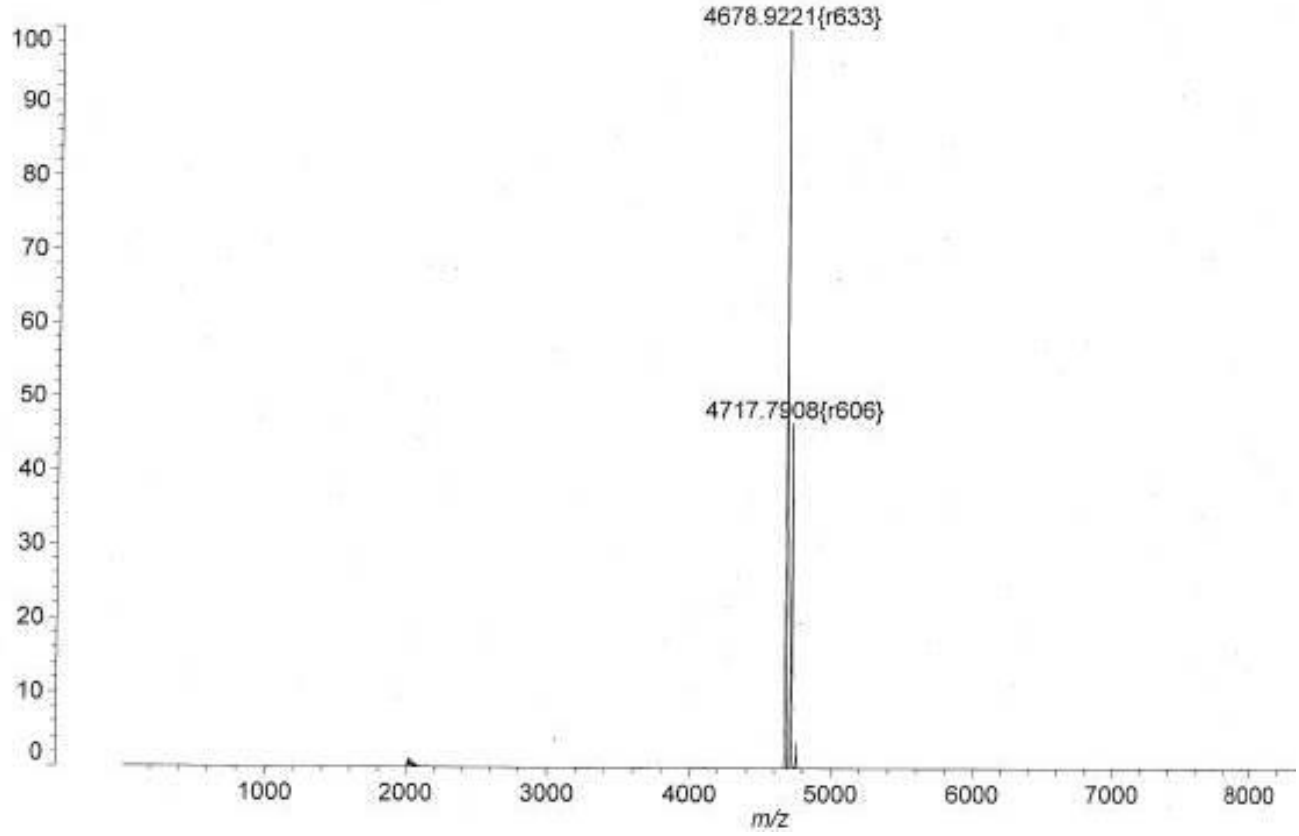

Figure S35: MALDI-TOF MS analysis of **DNA4b**: $M_{calc.}$ = 4681.5 g mol^{-1}, $M_{meas.}$ = 4678.9 g mol^{-1}.

4.4.3 Synthesis of DNA4

DNA4 (**Scheme S3**c) was obtained via a copper(I)-catalyzed alkyne-azide cycloaddition: **DNA4b** was dissolved in 50 µL ddH_2O and 57 µL of the azide-dye (10 mM in DMSO/^{t}BuOH 3:1), 34 µL tris-[(1-benzyl-1*H*-1,2,3-triazol-4-yl)methyl]amine (TBTA, 100 mM in DMSO/^{t}BuOH 3:1), 17 µL tetrakis(acetonitrile)copper(I)-hexafluorophosphate (100 mM in DMSO/^{t}BuOH 3:1) and 25 µL sodium ascorbate solution (400 mM in ddH_2O) were added. The solution was incubated for 2 h at 60 °C using a heating block. Subsequently, the solution was allowed to cool to ambient temperature and transferred into a 15 mL centrifuge tube. 450 µL sodium acetate (300 mM in ddH_2O) and 150 µL EDTA (50 mM in ddH_2O) were added and the conical centrifuge tube filled with 100% EtOH to a total volume of 10 mL. The solution was mixed on a vortex mixer and stored at -32 °C for 60 h. Subsequently, the solution was centrifuged for 10 min at 4000 rpm, followed by decantation of the supernatant. The remaining DNA pellet was washed 3x with 1 mL 80% EtOH by centrifugation for 10 min at 4000 rpm. The pellet was freeze dried and purified by HPLC (**Figure S36**) using a VDSphere, OptiBio PUR 300 S18-SE column (250×10 mm). **DNA4** was detected by a DAD-3000 diode array detector at 260 nm and 290 nm (DNA absorbance), 383 nm (SQ moiety absorbance) and 520 nm (Atto520 absorbance) and obtained as a red/purple powder.

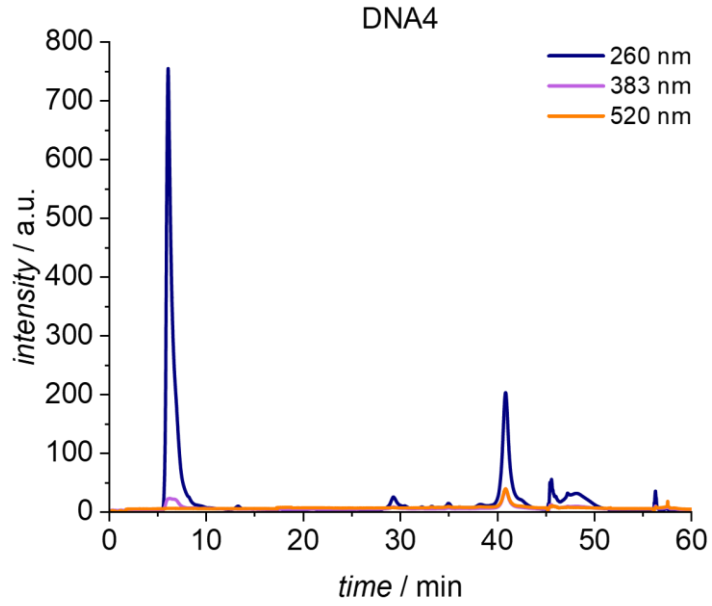

Figure S36: Semi-preparative HPLC analysis of **DNA4:** t_R = 40.8 min.

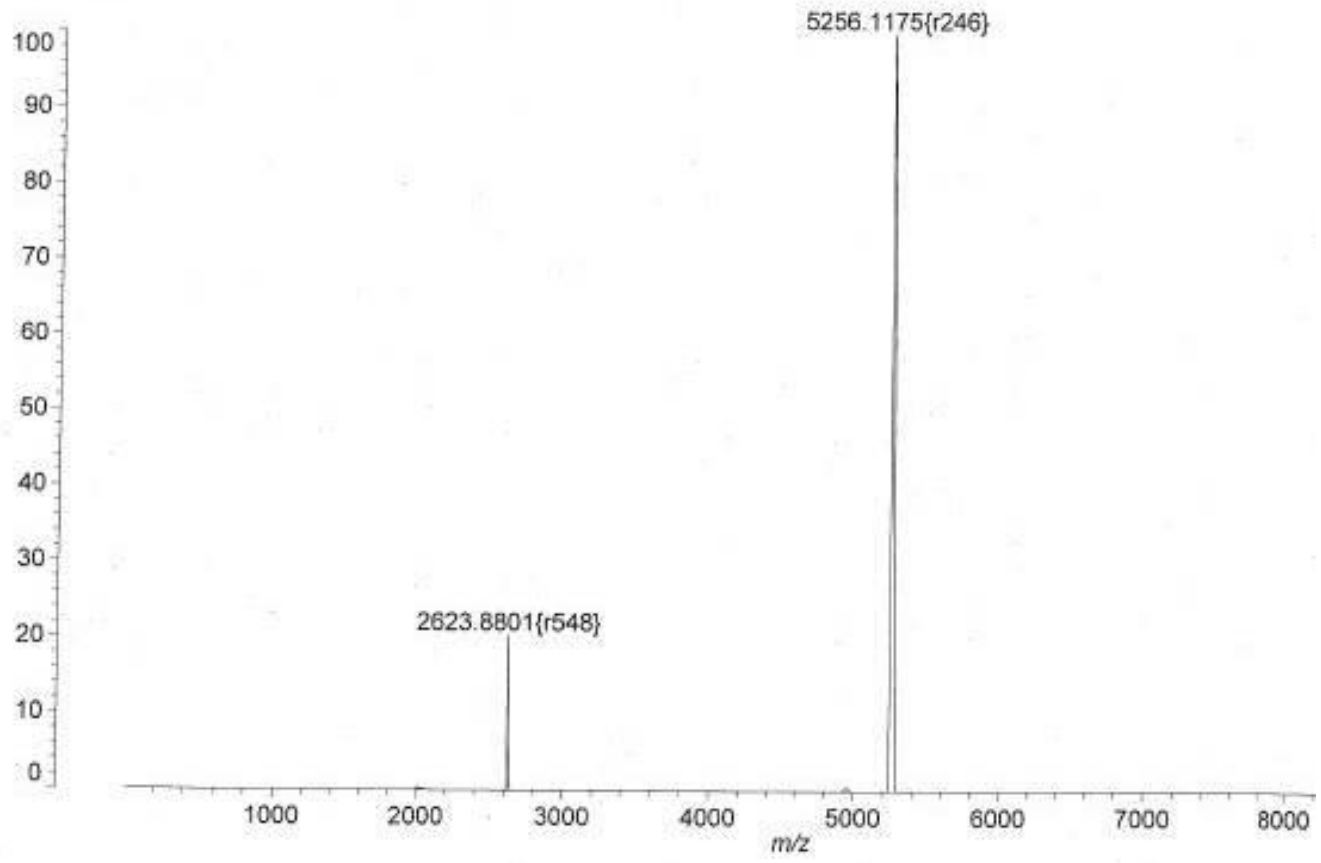

Figure S37: MALDI-TOF MS analysis of **DNA4**: $M_{calc.}$ = 5257.7 g mol^{-1}, $M_{meas.}$ = 5256.1 g mol^{-1}.

Oligonucleotide **DNA4** was quantified photometrically by absorption measurement at 260 nm at ND-100 spectrophotometer from Nanodrop and characterized via UV/Vis spectroscopy (**Figure S38**). **DNA4** shows four absorbance maxima in total: λ_{max1}=214 nm, λ_{max2} = 260 nm, λ_{max3}=383 nm and λ_{max4}=520 nm. λ_{max1} and λ_{max3} can be assigned to the SQ moiety, whereas λ_{max2} displays the typical DNA absorbance maximum and λ_{max4} the excitation maximum of the Atto520 dye.

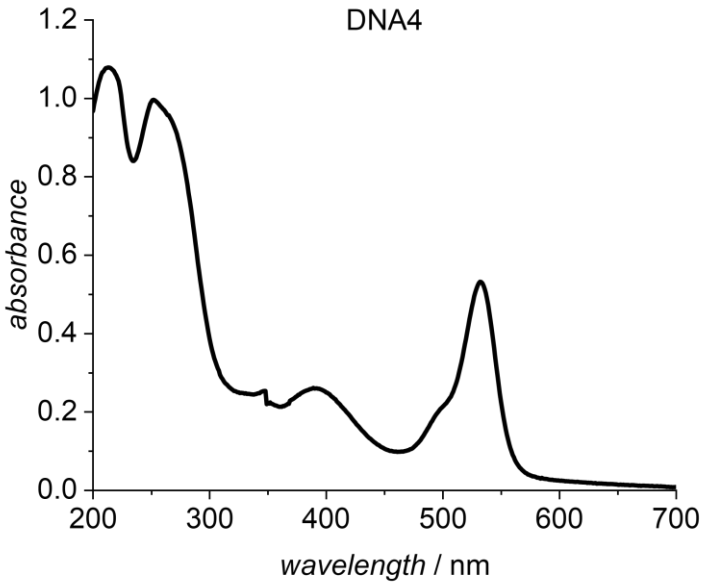

Figure S38: UV/Vis spectra of the oligonucleotide **DNA4**: 5 µM solution ddH_2O at 20 °C.

In addition, fluorescence spectroscopy of **DNA4** was performed (**Figure S39**). **DNA4** displays an emission maximum (orange line) at λ_{max}=550 nm when excited at λ_{exc}=488 nm.

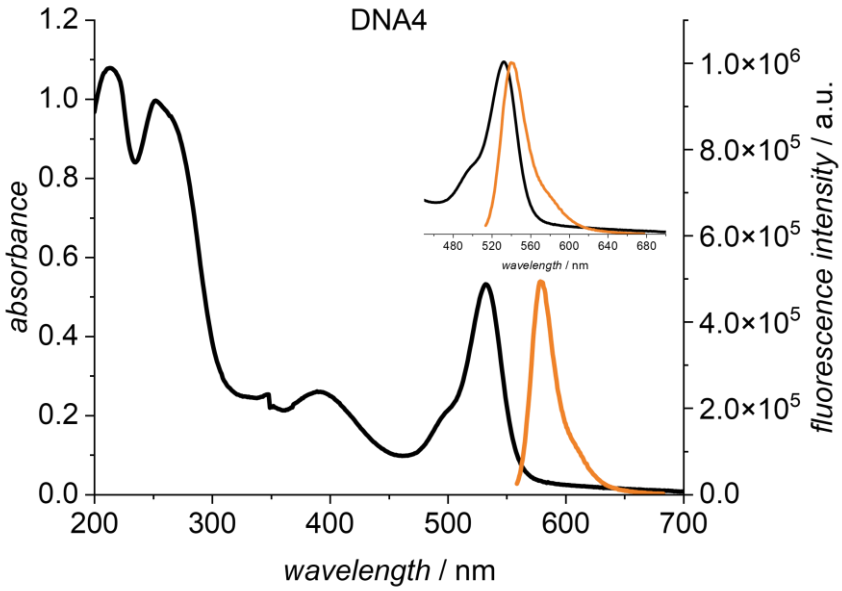

Figure S39: Emission spectra of the oligonucleotide **DNA4**: 5 µM solution ddH_2O at 20 °C, λ_{exc} = 488 nm, λ_{em} = 520-700 nm.

4.5 Synthesis and Analysis of DNA5

To further demonstrate the formation of **DNA5** (**Scheme S4**) as well as proving the concept for the performed cell experiments in solution, irradiation experiments with synthesized **DNA4** were performed *in vitro.*

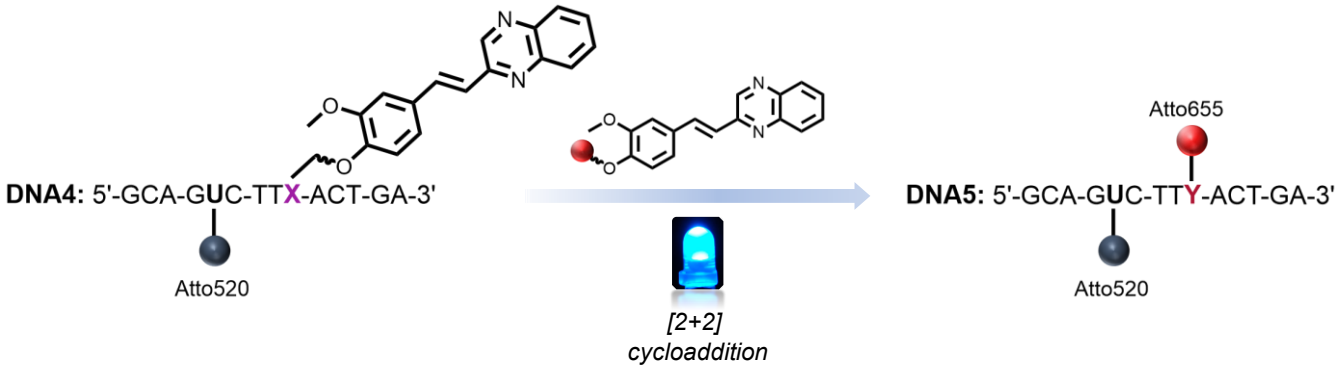

Scheme S4: [2+2] cycloaddition to hetero-dimerized **DNA5** through irradiation of 5 µM **DNA4** and 50 µM SQ-modified Atto655 dye **2** in aqueous solution, containing 5% DMSO, 10 mM Na-Pi buffer, 250 mM NaCl, pH 7 for 30 min at 37 °C using a 450 nm LED.

5 µM **DNA4** and 50 µM SQ-modified Atto655 dye **2** (stock solution in DMSO due to poor solubility in H_2O) in aqueous solution, containing 5% DMSO, 10 mM Na-P_i buffer and 250 mM NaCl in a total volume of 500 µL in a crimp vial were irradiated with a 450 nm LED for 30 min at 37 °C. LEDs (Duris E2835, GD JTLPS1.14) were purchased at Osram and the mixture was irradiated for 30 min from the bottom of the vial under continuous stirring and constant temperature of 37 °C. Heating of the reaction was performed using a Lauda Alpha R8 thermostat.
Afterwards, the samples were freeze dried over night and analyzed via denaturing PAGE. For better comparison, non-irradiated **DNA2** (monomer), **$(DNA2)_2$** (homo-dimer) and **DNA3** (hetero-dimer) samples were also applied on the same gel. Table S5 displays the sequences and masses of the synthesized oligonucleotides.

Table S5: Sequence and mass of synthesized oligonucleotides **DNA2, $(DNA2)_2$, DNA3, DNA4** and **DNA5**.

Probe	Sequence	M [g mol^{-1}]
DNA2	5'-GCA-GTC-TT**X**-TTC-ACT-GA-3'	5539.4
$(DNA2)_2$	5'-GCA-GTC-TT**X**'-TTC-ACT-GA-3'	11078.8
DNA3	5'-GCA-GTC-TT**Y**-TTC-ACT-GA-3'	6456.5
DNA4	5'-GCA-G**U**C-TT**X**-ACT-GA-3'	5257.7
DNA5	5'-GCA-G**U**C-TT**Y**-ACT-GA-3'	6174.8

The PAGE analysis (**Figure S40**) shows six lanes in total. Lane 1 displays non-irradiated **DNA2,** whereas lane 2 represents homo-dimerized **$(DNA2)_2$**. Lane 3 shows non-irradiated **DNA3** while lane 4 displays successful reaction of **DNA2** with SQ-modified Atto655 dye **2** to **DNA3** after 1 h of irradiation with a 450 nm LED. Gelelectrophoretic analysis of **DNA2, $(DNA2)_2$** and **DNA3** is discussed in further detail in the manuscript (refer to **Figure 2B** and **Scheme 2b**) and the ESI (**Figures S26, S27** and **S32**).
Lane 5 shows **DNA4** and lane 6 displays reaction of **DNA4** with SQ-modified Atto655 dye **2** to **DNA5** after 30 min of irradiation with a 450 nm LED at 37 °C. **DNA4** is expected to lead to a band with the fastest electrophoretic mobility as this sequence displays the lowest molecular weight. This is clearly confirmed through PAGE analysis, as lane 5 displays only one band with the fastest electrophoretic mobility. After successful reaction with SQ-modified Atto655 dye, **DNA5** features a mass between **DNA3** and **DNA4** (refer to Table S5) and is therefore expected to lead to a band with an electrophoretic mobility between these two fragments. Lane 6 clearly displays a fragment sized between **DNA3** and **DNA4**, clearly confirming the formation of **DNA5**. Despite the significant band for **DNA5**, lane 6 also displays two faint bands – one with a fast and one with a slow electrophoretic mobility. The lowest band can be assigned to starting material **DNA4**, whereas the other faint band shows homo-dimerization of **DNA4** to **$(DNA4)_2$**. Nevertheless, through 10-fold excess of Atto655 dye **2**, the reaction critically shows favourable reaction to hetero-dimerized **DNA5**. Furthermore, 30 min of irradiation time at 37 °C is sufficient to form the **DNA5** product.

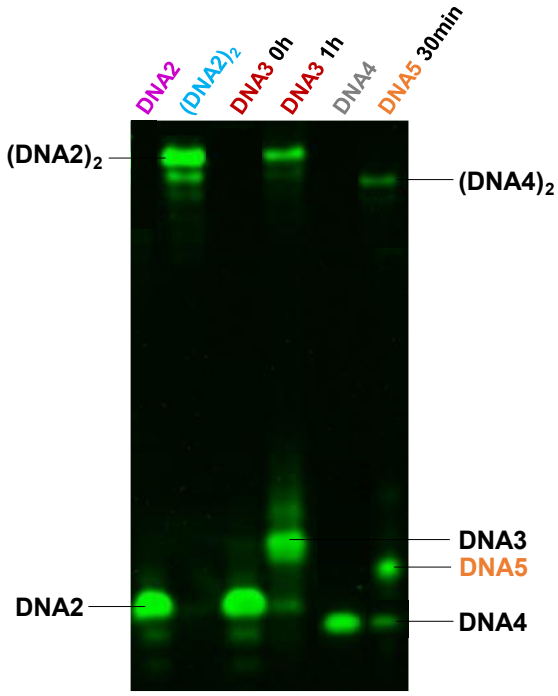

Figure S40: Denaturing PAGE analysis of **DNA5** after irradiation of 5 µM **DNA4** and 50 µM SQ-modified Atto655 dye **2** at λ_{max}=450 nm in aqueous media containing 5% DMSO, 10 mM Na-P_i buffer and 250 mM NaCl in a total volume of 500 µL in a crimp vial for 30 min at 37 °C. Staining was performed using SybrGreen, followed by visualization under UV light (λ_{exc}=312 nm). Lane 1: non-irradiated **DNA2**, lane 2: homo-dimerized **$(DNA2)_2$**, lane 3: non-irradiated **DNA3**, lane 4: **DNA3** after 1h of irradiation, lane 5: **DNA4**, lane 6: **DNA5.** Lane 6 shows a fragment sized between **DNA3** and **DNA4**, clearly confirming the formation of **DNA5** through visible light-induced [2+2] cycloaddition of SQ-modified **DNA4** and SQ-modified Atto655 dye **2**.

5 Cell Experiments

Human cervix carcinoma cells (HeLa) were bought from ATCC (Manassas Virginia) and cultured in Dulbecco's modified Eagle Medium (DMEM) containing 10% fetal calf serum and 1% penicillin/streptomycin (100 µg/mL at 37 °C / 5% CO_2). For subculturing, cells were detached with 0.25% trypsin-EDTA solution. For transfection, 4×10^4 cells per well were seeded into Ibidi 8-well µ-slides with ibiTreat surface. For cells, that were only treated with Atto655 dye and not transfected, 1×10^4 cells per well were seeded into Ibidi 8-well µ-slides with ibiTreat surface. Cells were seeded / transfected in Ibidi 8-well µ-slides as depicted in **Table S6**.

Table S6: Seeding / transfection protocol of HeLa cells in Ibidi 8-well µ-slides.

Cells	Atto655 control	Atto520 control	FRET
No **DNA4** No Dye	No **DNA4** Atto655 dye	**DNA4** No Atto655 dye	**DNA4** Atto655 dye
No **DNA4** No Dye	No **DNA4** Atto655 dye	**DNA4** No Atto655 dye	**DNA4** Atto655 dye

Cells were seeded into Ibidi 8-well µ-slides with ibiTreat surface and incubated for 24h. The next day, cells were transfected with 75 ng **DNA4** per well using ScreenFectA according to the protocol supplied by the manufacturer: Per transfected well, 1.4 µL ScreenFectA reagent was diluted with 38.6 µL dilution buffer. 1 µL **DNA4** (25.6 µM solution in water) was diluted with 39 µL dilution buffer. Both solutions were combined and incubated for 5 h to allow lipoplex formation. Subsequently, lipoplexes were diluted with 120 µL DMEM and the whole solution was added to the well. After incubation for 24 h, the cells were washed carefully 1x with PBS, followed by incubation for 16 h with 20 µM SQ-modified Atto655 dye **2** (4.41 mM stock solution in DMSO) in DMEM. Afterwards, the cells were again washed carefully 1x with PBS, covered with DMEM and irradiated with 450 nm LED for 30 min. The Ibidi 8-well µ-slide was irradiated from the bottom of the Ibidi at constant temperature of 37 °C. Heating was performed using a Lauda Alpha R8 thermostat.
Visualization of Atto520 and Atto655 dye was performed with a Leica DMi8, TCS SP8 confocal microscope with a 60x oil objective. Image acquisition was conducted at a resolution of 1024×1024 pixels and 8-bit depth using LAS X 3.5.7.23225 software. For Atto520 detection, excitation wavelength was set to λ_{exc}=488 nm (OPSL 488 laser, 20% laser power) and emission detected at λ_{em}=520-580 nm. Atto655 was excited at λ_{exc}=638 nm (OPSL 638 laser, 20% laser power) and emission measured at λ_{em}=665-750 nm, 20% laser power). For FRET detection, excitation wavelength was set to λ_{exc}=488 nm (OPSL 488 nm laser, 20% laser power) and emission detected at λ_{em}=665-750 nm. Fluorescence settings were complemented with a transmission channel, detected with a PMT detector.
It should be noted that for the live cell experiments, the stock solution of **2** was prepared in DMSO instead of DMF, caused by the solubility of **2**. DMF is cell toxic, whereas DMSO has sterilizing effect and does not affect the survival of the cells.

In addition, the following control experiments were performed:
1.) Negative control: No transfection with **DNA4**, incubation with 20 µM Atto655 dye **2** and irradiation at λ_{max}=450 nm

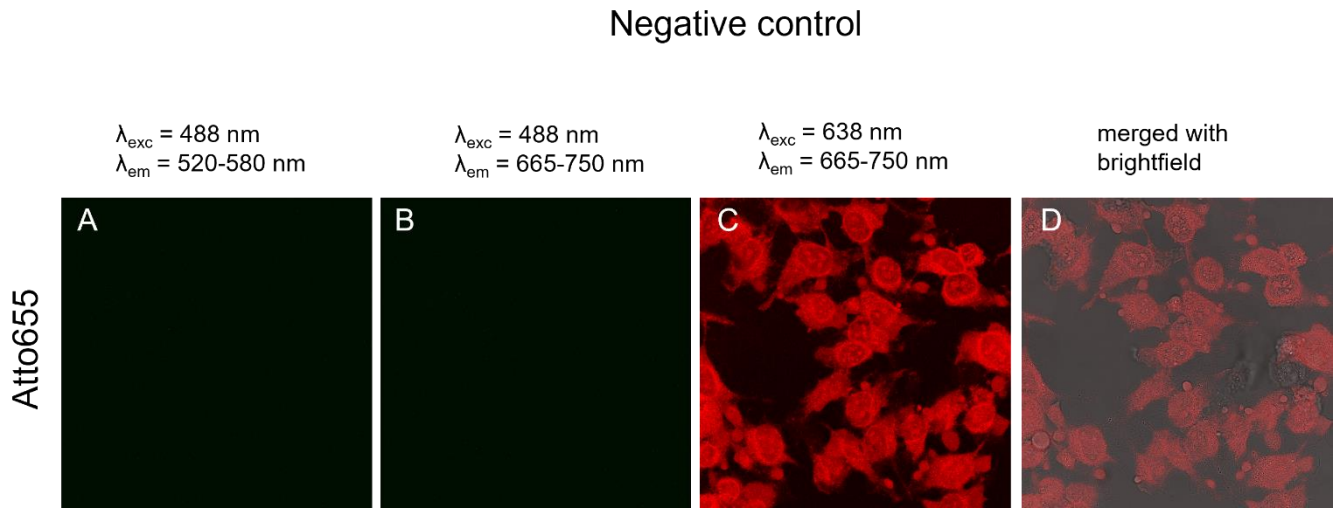

Figure S41: Confocal laser microscopy images of living *HeLa* cells, not transfected with **DNA4** but incubated with 20 µM Atto655 dye **2** for 16 h and irradiated with a 450 nm LED for 30 min at 37 °C.

As expected, the Atto655 dye shows fluorescence when excited at its respective excitation range (**Figure S41**C). Since the significant reaction partner (donor **DNA4** with Atto520-modification) for successful FRET is missing, no fluorescence at λ_{exc}=488 nm and λ_{em}=520-580 nm (**Figure S41**A) and λ_{exc}=488 nm and at λ_{em}=665-750 nm (FRET control, **Figure S41**B) is visible.

2.) Positive control: Transfection with **DNA3**

In addition to negative FRET controls (Manusrcript, **Figure 4**D-F and ESI, **Figure S41**A-D), positive controls were performed using **DNA3** which was irradiated and clicked before transfection: 4×10^4 cells per well were seeded into Ibidi 8-well µ-slides with ibiTreat surface and incubated for 24 h. The next day, cells were transfected for 24 h with 65 ng **DNA3** per well using ScreenFectA according to the protocol supplied by the manufacturer: Per transfected well, 1.4 µL ScreenFectA reagent was diluted with 38.6 µL dilution buffer. 1 µL **DNA3** (30 µM solution in water) was diluted with 39 µL dilution buffer. Both solutions were combined and incubated for 3 h to allow lipoplex formation. Subsequently, lipoplexes were diluted with 120 µL DMEM and the whole solution was added to the well. After incubation for 24 h, the cells were washed carefully 1x with PBS prior to confocal microscopy imaging at λ_{exc}=638 nm and emission detection at λ_{em}=665-750 nm. Significant fluorescence was clearly observable in the endosomes and the cytosol of the cells (**Figure S42**).

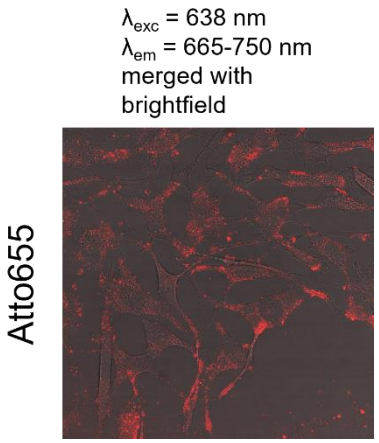

Figure S42: Confocal laser microscopy images of living *HeLa* cells, transfected for 24 h with 65 ng of **DNA3**. Imaging was performed at λ_{exc}=638 nm and λ_{em}=665-750 nm and confirmed successful labelling of *HeLa* cells using DNA that was irradiated and clicked before transfection.

6 References

1. K. Wada, J.-Y. Lee, H.-Y. Hung, Q. Shi, L. Lin, Y. Zhao, M. Goto, P.-C. Yang, S.-C. Kuo, H.-W. Chen and K.-H. Lee, *Bioorg. Med. Chem.*, 2015, **23**, 1507-1514.
2. K. Kalayci, H. Frisch, V. X. Truong and C. Barner-Kowollik, *Nat. Commun.*, 2020, **11**, 4193.
3. A. S. K. Hashmi, T. Häffner, W. Yang, S. Pankajakshan, S. Schäfer, L. Schultes, F. Rominger and W. Frey, *Chem. Eur. J.*, 2012, **18**, 10480-10486.
4. T. R. Battersby, D. N. Ang, P. Burgstaller, S. C. Jurczyk, M. T. Bowser, D. D. Buchanan, R. T. Kennedy and S. A. Benner, *J. Am. Chem. Soc.*, 1999, **121**, 9781-9789.
5. Á. Eördögh, J. Steinmeyer, K. Peewasan, U. Schepers, H.-A. Wagenknecht and P. Kele, *Bioconjugate Chem.*, 2016, **27**, 457-464.
6. K. Krell, B. Pfeuffer, F. Rönicke, Z. S. Chinoy, C. Favre, F. Friscourt and H.-A. Wagenknecht, *Chem. Eur. J.*, 2021, **27**, 16093-16097.
7. M. Merkel, K. Peewasan, S. Arndt, D. Ploschik and H.-A. Wagenknecht, *Chembiochem*, 2015, **16**, 1541-1553.